

**MODIFICATION AND RECOVERY OF THE SHOREFACE OF MATAGORDA
PENINSULA, TEXAS, FOLLOWING THE LANDFALL OF HURRICANE
CLAUDETTE: THE ROLE OF ANTECEDENT GEOLOGY ON SHORT-TERM
SHOREFACE MORPHODYNAMICS**

A Thesis

by

EDWARD JAMES MAJZLIK

Submitted to the Office of Graduate Studies of
Texas A&M University
in partial fulfillment of the requirements for the degree of
MASTER OF SCIENCE

May 2005

Major Subject: Oceanography

**MODIFICATION AND RECOVERY OF THE SHOREFACE OF MATAGORDA
PENINSULA, TEXAS, FOLLOWING THE LANDFALL OF HURRICANE
CLAUDETTE: THE ROLE OF ANTECEDENT GEOLOGY ON SHORT-TERM
SHOREFACE MORPHODYNAMICS**

A Thesis

by

EDWARD JAMES MAJZLIK

Submitted to the Office of Graduate Studies of
Texas A&M University
in partial fulfillment of the requirements for the degree of

MASTER OF SCIENCE

Approved as to style and content by:

Timothy M. Dellapenna
(Chair of Committee)

William R. Bryant
(Member)

Jay R. Rooker
(Member)

Wilford Gardner
(Head of Department)

May 2005

Major Subject: Oceanography

ABSTRACT

Modification and Recovery of the Shoreface of Matagorda Peninsula, Texas,
Following the Landfall of Hurricane Claudette: The Role of Antecedent Geology on
Short-Term Shoreface Morphodynamics. (May 2005)

Edward James Majzlik, B.S., University of South Carolina

Chair of Committee: Dr. Timothy M. Dellapenna

Matagorda Peninsula is located along an interfluvial region of the central Texas coast in the northwestern Gulf of Mexico. The Pleistocene Beaumont Clay underlies the coastal plain and inner continental shelf and controls the general slope of the coast in this region. This clay surface also creates low accommodation space for the preservation of modern sediments. As a result, only a thin (1 m) layer of transgressive Holocene muddy sand extends throughout the lower shoreface.

On 15 July, 2003, Hurricane Claudette (Category 1) made landfall on the peninsula. Following the storm, the shoreface was found to be an extensively eroded surface. Most obvious on this surface was an area containing numerous scour pits on the lower shoreface. These pits extended through the Holocene sediment and into the underlying Beaumont Clay. By the following July, the shoreface exhibited a relatively flat and featureless appearance. Rapid infilling of the pits was attributed to the high sediment supply to the area from converging longshore currents and by the relatively high accommodation space offered by the scoured areas.

A large amount of sediment was removed from the lower shoreface where the formation of scour pits occurred. This sediment would have been available for deposition

in storm layers both inshore and offshore of the scoured area. Within scour pits, accommodation space was high, resulting in sediment deposition and rapid infilling of the pits. Outside of the scour pits, accommodation space remained low and sediment deposition did not occur. Preservation potential of the sediment record on the shoreface was low and was controlled by cycles of erosion and deposition during storm events. Antecedent geology of the shoreface and the sedimentary processes occurring during and after the storm supported arguments against the assumptions used by the classic "profile of equilibrium" model. Finally, the heavily scoured surface represents a geohazard to development of nearshore regions.

ACKNOWLEDGEMENTS

Funding for this project was provided the Texas General Land Office through the National Oceanic and Atmospheric Administration's Coastal Management Program and by the Geological Society of America, Graduate Study Research Grant #7734-04.

Special thanks go out to the members of the Coastal Geology Lab at Texas A&M Galveston, especially to Julie Manuel, Andrew McInnes, Nicole Joiner, Bryan Fielder, Christian Noll, and Dr. Ansley Wren for their extensive support with the collection of data in the field, analysis of the data in the lab, and help with preparation of this manuscript.

Thanks to Bob and Willis, the crew of the R/V *Eugenie*, Dr. Mead Allison and Jeff Nittrouer from Tulane University's Department of Earth and Environmental Sciences for their contributions during the initial cruise to Matagorda Peninsula and for their continued support with data analysis and manuscript preparation, Beth Friesner at the Galveston Veterinary Clinic for her help x-raying the sediment cores, and the Virginia Institute of Marine Science's Department of Physical Sciences for the generous use of their sediment lab.

Finally, thanks to my advisor and friend, Dr. Tim Dellapenna, for the many opportunities and adventures in oceanography and for the countless lessons both in and out of the lab.

TABLE OF CONTENTS

	Page
1. INTRODUCTION.....	1
2. MATAGORDA PENINSULA.....	3
3. HURRICANE CLAUDETTE.....	6
4. METHODS.....	8
4.1 Sidescan Sonar.....	8
4.2 Bathymetry.....	9
4.3 Chirp Seismic Sonar.....	10
4.4 Gravity Cores.....	10
4.5 Surface Sediment Grabs.....	11
4.6 Wave and Current Analysis.....	12
5. RESULTS.....	14
5.1 Sidescan and Multibeam Sonar.....	14
5.2 Seismic Sonar.....	22
5.3 Surface Sediment Samples.....	24
5.4 Sediment Cores.....	28
5.5 Waves and Combined Flow.....	30
6. DISCUSSION.....	31
6.1 Mechanisms for Shoreface Scouring.....	31
6.1.1 Waves.....	31
6.1.2 Currents.....	31
6.2 Formation of Shoreface Scours.....	34
6.3 Recovery of the Shoreface.....	38
6.4 Implications for the Inner Continental Shelf.....	40
6.4.1 Transgressive Layer Dynamics.....	40
6.4.2 Implications for “Profile of Equilibrium”.....	40
6.4.3 Geohazards.....	42
7. CONCLUSIONS.....	45
REFERENCES.....	48
APPENDIX A.....	54
APPENDIX B.....	58

	Page
APPENDIX C.....	60
VITA.....	64

LIST OF FIGURES

FIGURE	Page
1 Matagorda Peninsula study area and location along the Texas coast.....	5
2 Storm track for Hurricane Claudette.....	7
3 Sidescan sonar mosaic from July 2003 following the landfall of Hurricane Claudette.....	15
4 Multibeam sonar bathymetry data collected in July 2003.....	15
5 Sidescan sonar image and multibeam bathymetry of shore-normal channels found on the sandy upper shoreface.....	17
6 Sidescan sonar image and multibeam bathymetry of clay floored scour pits found on the lower shoreface.....	18
7 Sidescan sonar image and multibeam bathymetry of muddy sand floored scour pits found on the lower shoreface.....	19
8 Sidescan sonar mosaic from January 2004.....	20
9 Sidescan sonar mosaic from July 2004.....	20
10 Change in bathymetry between July 2003 and July 2004.....	21
11 Bathymetric profile measured during each survey.....	22
12 Shore normal Chirp profile showing the stratigraphic surfaces within the shoreface.....	23
13 Chirp seismic data across a series of clay floored scour pits on the lower shoreface.....	24
14 Surface sediment grain size distribution for July 2003 and location of gravity cores.....	25
15 Surface sediment grain size distribution for January 2004 and location of gravity cores.....	26
16 Surface sediment grain size distribution for July 2004 and location of gravity cores.....	27

FIGURE	Page
17 Grains size distribution profiles and x-rays for all three cores.....	29
18 Time-series bottom shear stress velocities calculated for 8 m water depth.....	30
19 Sidescan sonar images from July 2003.....	44

1. INTRODUCTION

The shoreface environment is a region of extreme sensitivity to variations in sediment supply, sea-level, and hydrodynamic processes (Rodriguez et al., 2001). Intense, short time-scale modifications to each of these parameters are possible during the landfall of a hurricane. These short time-scale events are often the cause of the most dramatic and obvious changes in the nearshore sedimentary environment (Wright, 1995), with recovery times often on the scale of months to years (Schwarzer et al., 2003).

The enormous power a hurricane imparts to the seafloor of the shoreface and inner continental shelf is an important mechanism for extensive transport of sand from the shoreface and reworking of nearshore bathymetry (Gayes, 1991). During these large storms, the rate of sediment transport on the shoreface increases by at least an order of magnitude (Swift et al., 1985).

The evolution of the shoreface during a hurricane impact is not controlled by hydrodynamic forces alone. The role of antecedent geology is crucial in determining the response of the shoreface to increased hydrodynamic forcing (Belknap and Kraft, 1985). Antecedent geology controls the regional slope of a coastline. In the case of coastal barrier complexes, such as the one found at the study site, the slope of the coastline is controlled by the surface of the pre-Holocene sediment unit. The depth of this surface directly affects the thickness of Holocene sediments above it (Belknap and Kraft, 1985).

This thesis follows the style and format of Marine Geology.

During a hurricane, both intense wave orbital currents and wind-driven flow are capable of mobilizing and transporting sediment from the shoreface (Swift et al., 1985). This transport may move large amounts of sediment in on- and offshore directions. Offshore directed bottom currents may deposit sediment on the adjacent inner continental shelf (Niedorado et al., 1985), while strong onshore currents may transport material from far offshore and deposit it on subaerial portions of the coast (Hayes, 1967).

The shoreface of Matagorda Peninsula, Texas, was impacted by the extreme forces mentioned above during the landfall of Hurricane Claudette. This study attempts to document the geologic response of the shoreface to the hurricane in order to understand the forces present during landfall and the role of antecedent geology on the expression of the shoreface response. During the following year, the shoreface was observed to determine the processes and time-scales involved in the recovery of the shoreface to a fair-weather configuration. Also, observations were made to determine the effect of previous hurricane impacts to shoreface within the study area.

2. MATAGORDA PENINSULA

Matagorda Peninsula is located along the central Texas coast at 28.6° N and 95.9° W (Figure 1). The peninsula is roughly 84 kilometers long and 2 kilometers wide at its widest point, near the Colorado River delta, where it crosses Matagorda Bay. The peninsula was formed during the most recent transgression of sea level 5000 years ago, around the time of the formation of other coastal barriers in Texas (Bernard et al., 1970; Rodriguez et al., 2004). The Pleistocene age Beaumont Clay underlies the Holocene age sediment of the peninsula. The Beaumont Clay acts as a foundation to the coastal plain, and is composed of stiff orange clay with shear strengths exceeding 1 kg cm⁻². Radiocarbon dates from exposed Beaumont Clay yield ages ranging from 37,080 to > 46,160 year BP (Rodriguez et al., 2001).

Despite the presence of the Colorado River, the study area was located on an interfluvial region of the central coast. Interfluvial areas were defined by Rodriguez et al (2001) as areas where "modern shoreface deposits prograde directly over Pleistocene deposits." In these areas, accommodation space for modern sedimentation is kept low by the shallow surface of the Beaumont Clay.

Upper shoreface sand on Matagorda Peninsula extend for less than 1 km offshore and is very fine sand with a modal grain size of 0.088 mm (3.5 ϕ). The upper shoreface has a slope of 3.25 m km⁻¹, extending to a depth of 7 m. Offshore of the 7 m isobath, the lower shoreface is covered by increasingly muddier sand and has a slope of 0.97 m km⁻¹. The lower shoreface sediments create a thin veneer of material (up to 1 m thick within 3 km of shore) covering the Beaumont Clay ravinement surface. The inner continental shelf sediments of central Texas are characterized by a marine mud unit containing

discrete storm event layers of very fine sand and silt typically ranging in thickness from 1 to 10 cm (Rodriguez et al., 2001).

The Texas shoreline has been classified as a microtidal, wave dominated coast with a diurnal tidal range of 0.65 m (Hayes, 1979). Hindcast wave heights for 20 years by Hubertz and Brooks (1989) indicated a mean significant wave height of 1 m at a location 40 km southeast of the Colorado River mouth in 26 m of water. Hayes (1967) reported that the frequency of tropical storms crossing the Texas coast was 0.67 storms per year. A mean significant wave height of 5.1 m has a return interval of five years due to tropical storm activity along the Texas coast (Abel et al., 1989).

The central Texas coast has the highest sediment supply on the Texas coast due to converging longshore currents flowing into this region from south and east Texas (Rodriguez et al., 2001). Although a distributary of the Colorado River empties into the Gulf of Mexico through Matagorda Peninsula, no subaerial delta has formed and the shoreface is dependant on distal sources of sediment (such as longshore drift) for shoreline maintenance (McGowen and Scott, 1975).

The peninsula is subject to inundation during tropical storm events and numerous storm washover fans have been mapped along the length of the peninsula (Gibeaut et al., 2000). Three storm surge/tidal inlets are present and these inlets are subject to opening following the passage of tropical storms (Gibeaut et al., 2000). The breach at Three Mile Lake (Figure 1) is the closest storm surge inlet to the study area and was opened by Hurricane Claudette.

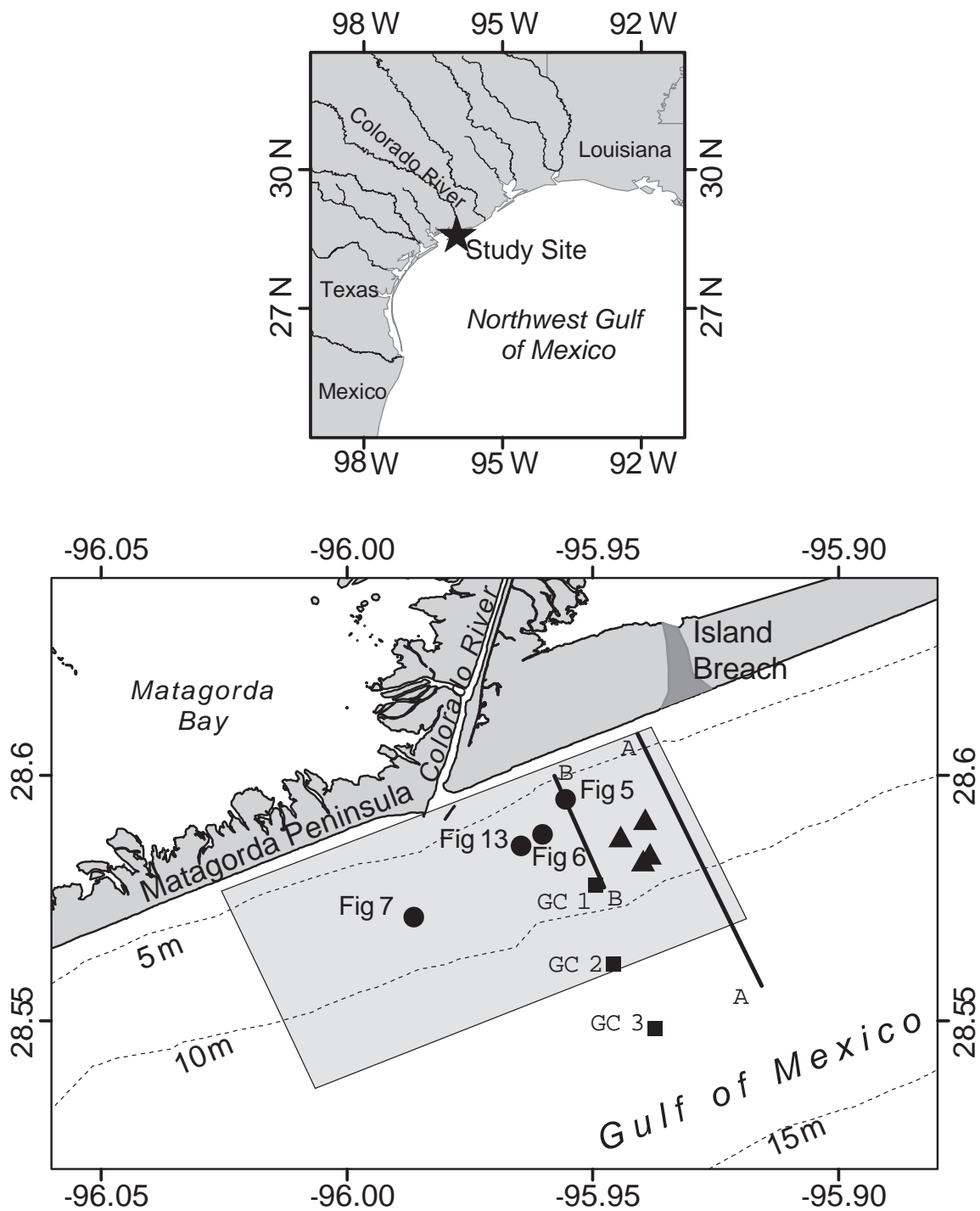


Figure 1: Matagorda Peninsula study area (shaded box) and location along the Texas coast. Locations of gravity cores (squares), oil platforms (triangles), Chirp and bathymetry profiles, Figures 5, 6, 7, and 13, and the island breach at Three Mile Lake are noted.

3. HURRICANE CLAUDETTE

Hurricane Claudette (Figure 2) began as a tropical wave off the coast of western Africa on 1 July, 2003. By 7 July, the tropical wave had entered the Caribbean Sea and was upgraded to Tropical Storm Claudette. On 11 July, Claudette made her first landfall on Mexico's Yucatan Peninsula before entering the Gulf of Mexico with sustained winds of 26 m s^{-1} . During the next four days, the storm gathered strength and became a Category I hurricane shortly before landfall on the Texas coast (Beven, 2003). Mean wave heights of 5.5 m were reported around 0100 h on 15 July, 2003, by the National Data Buoy Center (NDBC) buoy 42019, located 35 km southwest of the eye of the hurricane in 83 m of water (National Data Buoy Center, 2003). On 15 July, 2003, the storm made landfall on Matagorda Peninsula with sustained winds of 41 m/s and a central pressure of 979 mb. By the following day, Claudette had weakened to a tropical storm and was rapidly moving westward into Mexico (Beven, 2003). The rapid movement of the storm inland limited rainfall totals and only minor flooding was reported. A storm tide of 2.4 m was recorded at the Colorado River Locks in Matagorda, 11 km upstream from the mouth of the river (Beven, 2003). Nation Ocean Service (2003) tide gauges in Freeport and Rockport, TX, 76 km east and 123 km west of Matagorda, recorded storm tides of 2.1 m and 0.6 m, respectively, above mean lower low water level.

4. METHODS

The study site was located offshore of Matagorda Peninsula, Texas, along the stretch of coast where the most intense winds of Hurricane Claudette made landfall. The site extended for 5 km in either direction along the coast from the mouth of the Colorado River (Figure 1). It extended across the shoreface from nearly 2 m water depth out to 10 m water depth (about 3 km from shore).

Three cruises were conducted at the study area at two weeks (July 2003), six months (January 2004), and one year (July 2004) after the hurricane made landfall. The initial survey was timed to document the effects of the hurricane on the seafloor geology. The following two surveys were designed to observe the seafloor as it transitioned back to a fair-weather state.

Due to time and budget constraints, the extent of the survey area for the subsequent cruises only included the northeastern half of the initial surveyed area. This location was chosen for further investigation due to the more heavily eroded seafloor found in the northeastern half of the initial survey area.

4.1 Sidescan Sonar

Sidescan sonar operates by measuring the intensity of reflected sound from the seafloor. The intensity of the echo is a function of seafloor composition. Higher echo intensity results where the seafloor is harder or composed of coarser grained sediment. Lower echo intensity results where the seafloor is composed of softer or finer grain sediment. Echo intensity is then displayed as areas of lighter (higher echo intensity) or darker (lower echo intensity) colored pixels by the acquisition software.

Ensonification of the seafloor was completed using an Edgetech 272TD sidescan sonar towfish operating at 100 kHz. Survey line spacing and sidescan sonar ranges varied from 100 to 150 m. The incoming sonar data were acquired and saved using CodaOctopus geosurvey software. This software geocoded the sonar images to navigation data supplied by a differentially corrected Trimble GPS receiver. Layback between the towfish and the GPS antenna was calculated and applied to the final corrected towfish position. Following the surveys, the sidescan sonar data were geocoded and mosaiced using the software. The mosaics were then read into ArcGIS software and notable seabed features were identified in each mosaic. The presence and location of these features were compared between the three surveys in order to track the changes to the seafloor.

4.2 Bathymetry

Bathymetry data were also collected during the three cruises. The first cruise used a pole-mounted Reson 8101 multibeam sonar to gather swath bathymetry data with centimeter-level precision. The multibeam sonar data were acquired using Caris Hydrographic Information Processing Software (HIPS). This software also geocoded individual depth soundings and applied vessel heave, pitch, and roll corrections supplied by a TSS model 320 POS/MV system. Caris HIPS software was also used to process data to remove spurious data and to tide correct readings to the MLLW datum. Corrected data were then converted into raster format.

The subsequent two cruises both used an Odom Hydrotrac 200 kHz, singlebeam sonar to obtain bathymetry data along the survey track lines. Singlebeam data were

acquired and geocoded using Hypack Max Survey software. The singlebeam data were processed using Hypack Max Singlebeam Editor software to remove spurious data and to tide correct the data to the MLLW datum. The edited singlebeam data were then converted into raster data using ArcGIS software. Within the ArcGIS software, the bathymetry grids were compared to measure bathymetry changes between surveys.

4.3 Chirp Seismic Sonar

Chirp seismic sonar data were collected using an Edgetech 216S Full Spectrum Sub-Bottom towfish. Chirp seismic system used a signal ranging in frequency from 2 to 16 kHz to produce decimeter resolution data of the upper sediment column. Seismic data were acquired and geocoded using DelphSeismic Plus software. Seismic data were collected concurrently with sidescan sonar acquisition during the July 2003 cruise. These data were then processed using DelphMap and SeismicGIS software to determine the thickness of the Holocene sediment layer throughout the survey area. Selected areas were surveyed using the Chirp again in July 2004 to examine shoreface sediments during their recovery.

4.4 Gravity Cores

Three gravity cores were recovered during the July 2003 cruise. Cores were taken from the continental shelf in water depths of 8.7, 11.4, and 12.5 m (Figure 1). X-radiographs of the cores were made using a Duocon 1 machine set at 74 keV and 80 mAmp s⁻¹. Cores were x-rayed in 17 cm long sections. Developed x-rays were scanned into digital format using Adobe Photoshop and mosaiced using Adobe Illustrator

software to reconstruct entire cores. The x-ray images enabled observations of the sedimentary fabric of the core samples and enabled reconstruction of the depositional history of the cores. Rapid or pulsed deposition was characterized by discrete, highly laminated sequences. Slower, steadier deposition was characterized by a mixed sequence containing no discrete layers. General sediment grain size could also be determined by the x-rays. Lighter areas represented coarser sediment and darker areas represented finer sediment.

After the full round cores were x-rayed, they were split and subsampled at 1 cm intervals. Sediment grain size distribution was determined for the odd numbered subsamples throughout each core following the method described by Folk (1954). This analysis determined the percentage by mass of sand, silt, and clay sized particles in each sample. These data were then entered into spreadsheet format and plotted against depth to create sediment grain size profiles. Further analysis of the distribution of sand sizes was carried out on selected samples using the Rapid Sediment Analyzer (RSA) located at the Virginia Institute of Marine Science (VIMS). The RSA method determines sediment grain size by applying an empirical equation that relates the settling velocity of sand grains through a settling column to sediment grain size (Gibbs et al., 1971).

4.5 Surface Sediment Grabs

Surface sediment grab samples were recovered throughout the survey area during all three cruises. Two sampling devices were used on the July 2003 cruise during which 26 samples were recovered. These were a hand deployed Ponar grab and a larger winch deployed, spring loaded Smith-McIntyre grab. The Ponar was used to recover samples

from muddier sediment, while the Smith-McIntyre was used to recover samples in coarser sediment. The January and July 2004 cruises both employed the hand operated Ponar grab to recover 25 and 15 samples, respectively. A subsample of the each sediment grab was kept for grain size analysis using the Folk (1954) method. Percentages of sand, silt, and clay were then loaded into a GIS program to map the distribution of surface grain sizes and to ground-truth the sidescan sonar data. RSA analyses of the surface grabs were used to determine the modal grain size of the sand found throughout the study area.

4.6 Wave and Current Analysis

Wave height and period data collected at NOAA buoy 42019 during the passage of Hurricane Claudette were used to calculate a time-series of bottom shear velocities at the 8 m water depth during the landfall of the storm. Bottom shear velocities for wave (U_{*wm}), current (U_{*c}), and combined (U_{*cw}) flows were calculated using the algorithms of Styles and Glenn (2000). Although no current measurements were recorded during Hurricane Claudette's landfall, an onshore bottom current of 1 m s^{-1} was assumed to calculate U_{*c} and U_{*cw} . A similar current was measured by Allison et al. (in review) during the landfall of Hurricane Lili (2002) in Louisiana. The Styles and Glenn (2000) model also calculated the critical shear velocity (U_{*cr}) for the 0.088 mm sand found throughout the study area.

Location of the breaking waves was calculated based on the empirical relationship described in the Shore Protection Manual (U.S. Army, 1984) for spilling breakers. The actual position of the breaker depth was then adjusted to account for the effect of the

storm surge. This location was compared to the sidescan and multibeam sonar data from July 2003.

5. RESULTS

5.1 Sidescan and Multibeam Sonar

Sidescan and multibeam sonar data from July 2003 revealed an extensively eroded seafloor throughout the survey area (Figures 3 and 4, respectively). This surface was composed of three distinguishable features. First, shore-normal channels were located on the upper shoreface between 3.5 and 6.5 m water depth (Figure 5). The channels ranged in depth from 0.25 to 0.40 m and width from 25 to 55 m. The channels were floored with the same sand that comprised the upper shoreface. This resulted in a relatively weak contrast in the sidescan sonar data to unchanneled areas of the shoreface.

Second, scour pits floored with exposed Beaumont Clay were located between 7 and 9 m water depth (Figure 6). These features were most prevalent in the northeastern half of the study site. These pits displayed the highest relief of the three features, ranging in depth from 8 to 103 cm (Table 1). Debris fields extended directly offshore from many of the pits (Figure 6). The shoreward extent of this region was delineated by a shore-parallel belt of exposed Beaumont Clay. This belt extended intermittently throughout the entire study area marking a transition from channelized to scour pit erosion. This belt also marked the location of a break in slope from 3.25 m km^{-1} to 0.97 m km^{-1} . Clay floors of the scour pits appeared in sharp contrast in the sidescan sonar data to the muddy sand which surrounded the scour pits.

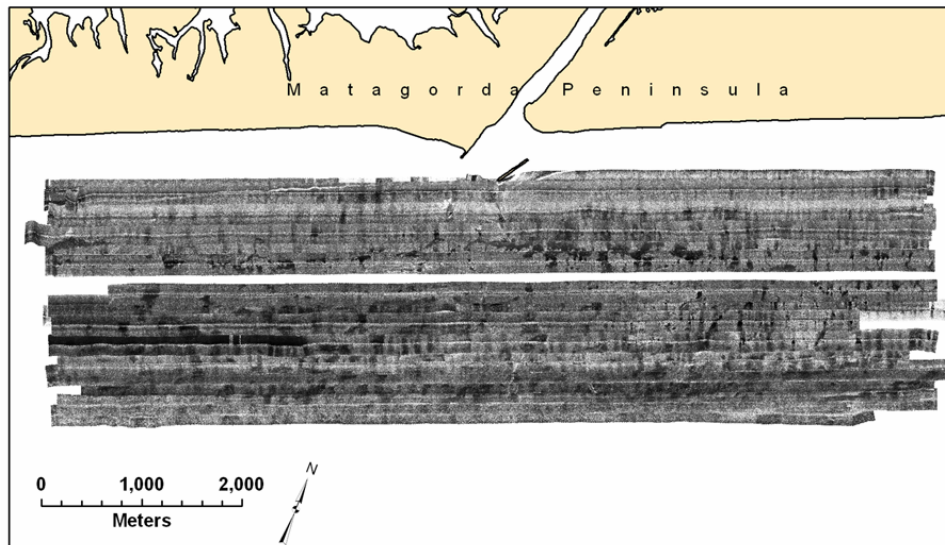


Figure 3: Sidescan sonar mosaic from July 2003 following the landfall of Hurricane Claudette. Dark colors represent areas of lower acoustic return found within the clay floored scour pits.

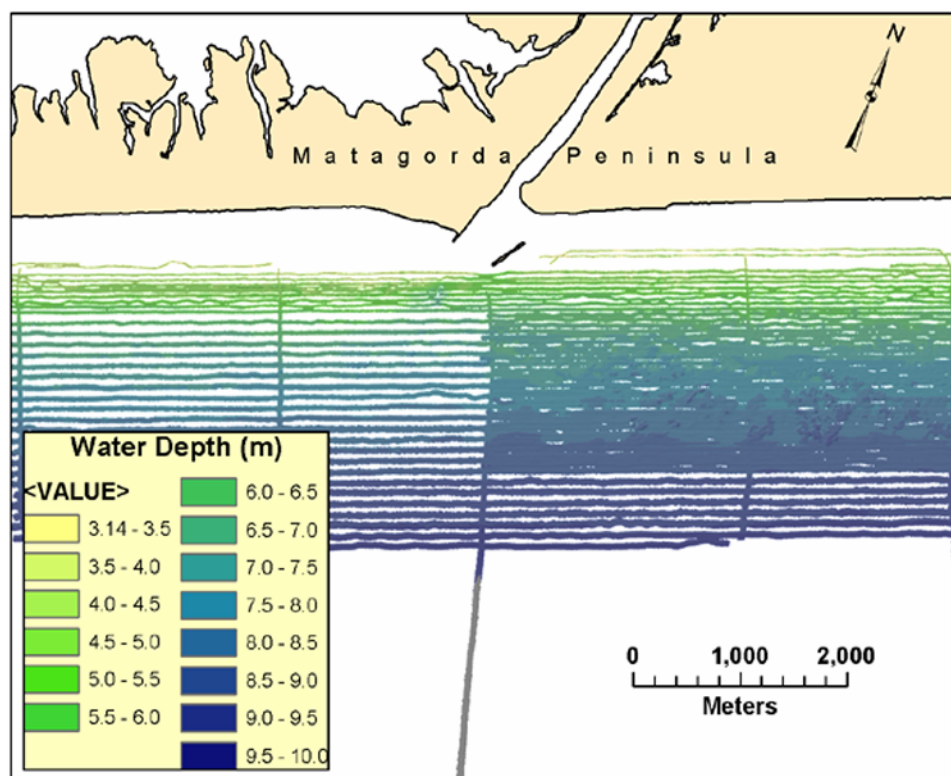


Figure 4: Multibeam sonar bathymetry data collected in July 2003. The overall gentle slope of the shoreface exhibited areas of high relief where large pits had been scoured up to 1 m into the seafloor.

Third, scour pits floored with the same muddy sand that surrounded them were located from 7 m to the offshore extent of the survey, in 10 m water depth (Figure 7). They occurred along the length of the study area, except where the clay floored pits occurred. These pits ranged in depth from 0.1 to 0.2 m. These features also had a relatively weak contrast to surrounding sediment in the sidescan sonar data.

By January 2004, the only features still visible in the sidescan sonar data (Figure 8) were remnants of the exposed Beaumont Clay belt. Channels located on the shoreface had transformed into a relatively flat and featureless surface. The scour pits located offshore were no longer clearly delineated and the sharply contrasting Beaumont Clay surface was no longer visible. Singlebeam echosounder data collected directly over the former location of selected scour pits showed that pits had been completely filled.

Sidescan sonar data from July 2004 contained a large low-backscatter anomaly in the general area of the exposed clay belt (Figure 9). The scoured area offshore of the clay belt was characterized by a mottled pattern of high and low backscatter. The lower backscatter patches of this pattern occurred in the general area of the heaviest scour from the previous July. Once again, echosounder data in this area revealed no evidence of the former scouring.

Table 1

Clay floored scour pits

Scour pit size and depth summary

	Min	Max	Mean	Std. Dev.
Area (m ²)	4.7	9370.0	1051.6	1503.9
Depth (cm)	8	103	54.2	21.4

Pit coverage within scoured region = 6.46%

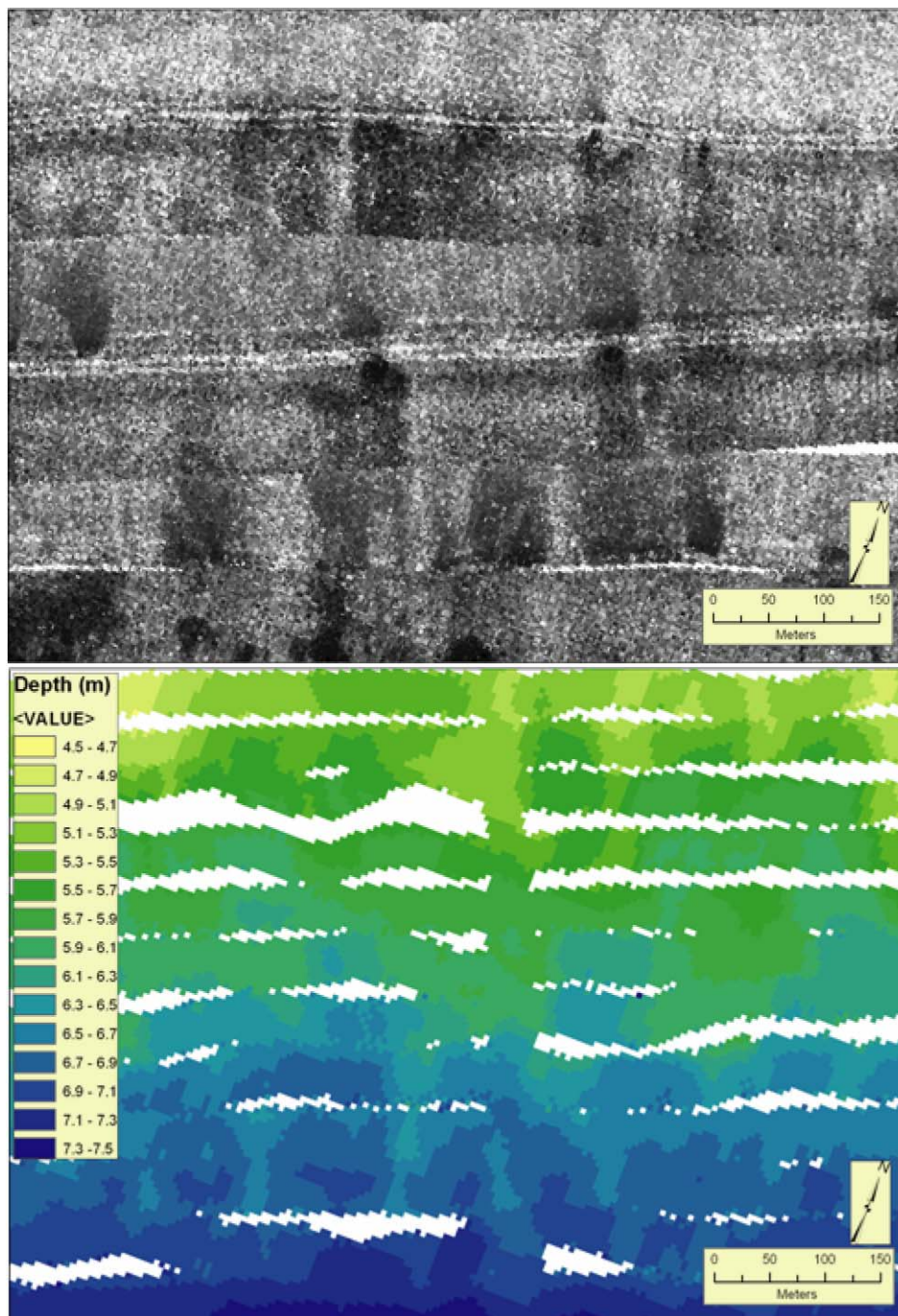


Figure 5: Sidescan sonar image (top) and multibeam bathymetry (bottom) of shore-normal channels found on the sandy upper shoreface.

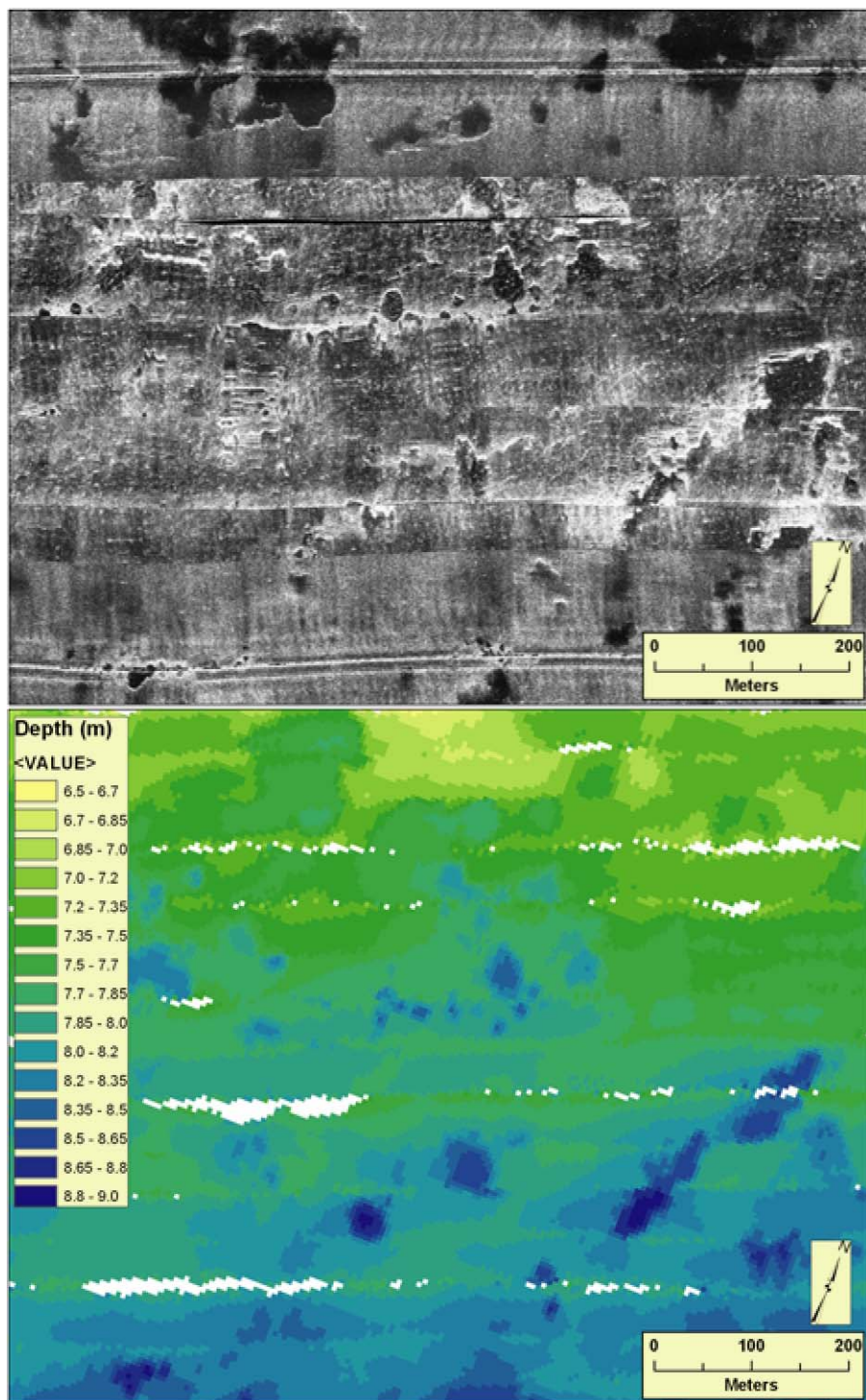


Figure 6: Sidescan sonar image (top) and multibeam bathymetry (bottom) of clay floored scour pits found on the lower shoreface.

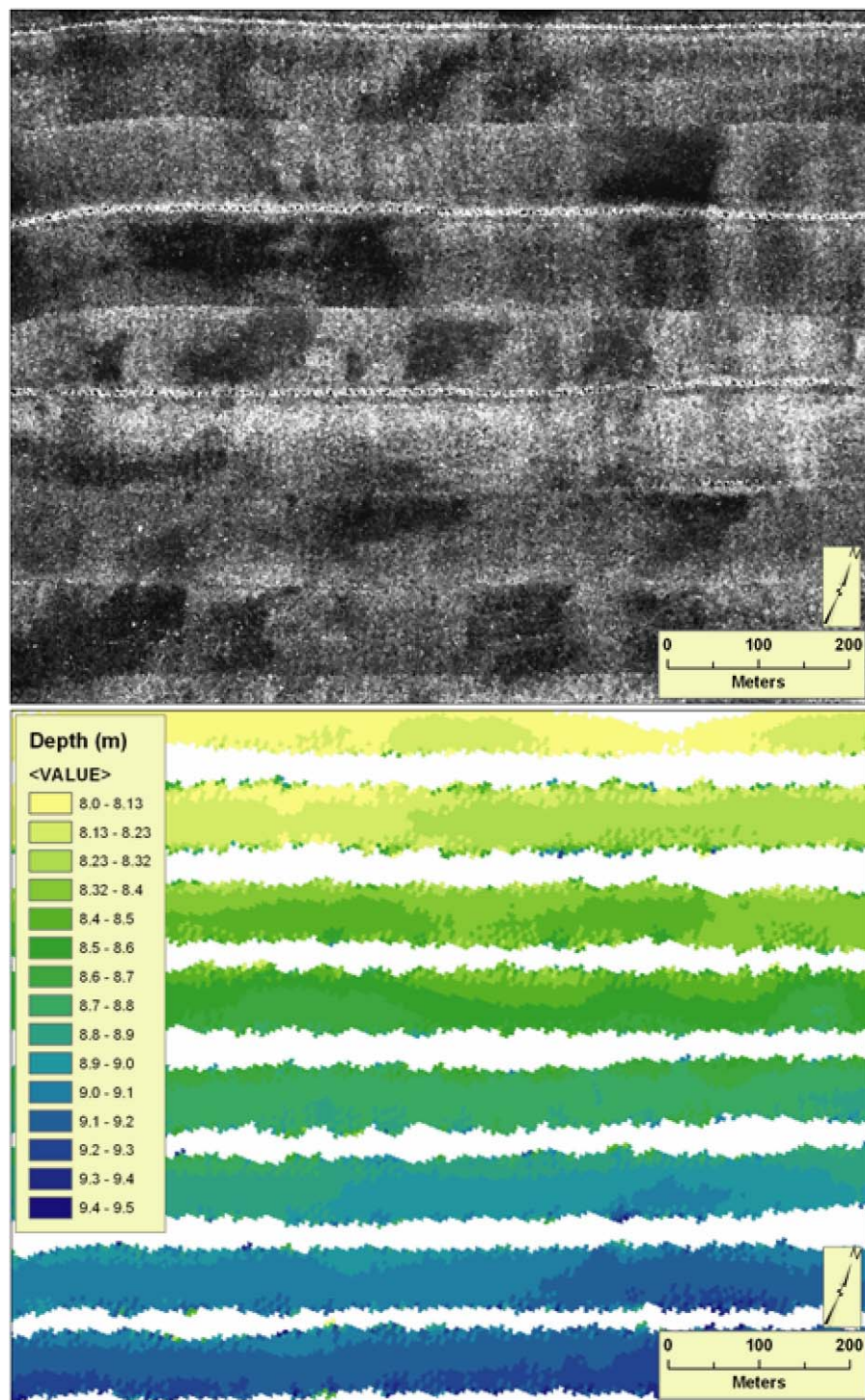


Figure 7: Sidescan sonar image (top) and multibeam bathymetry (bottom) of muddy sand floored scour pits found on the lower shoreface.

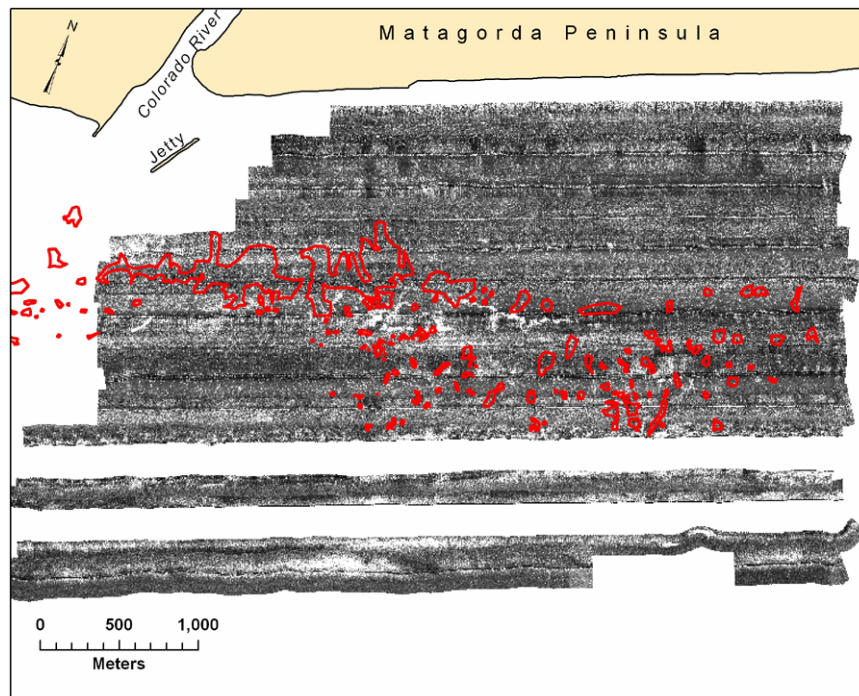


Figure 8: Sidescan sonar mosaic from January 2004. Outlined areas indicate the location of exposed Beaumont Clay found in July 2003.

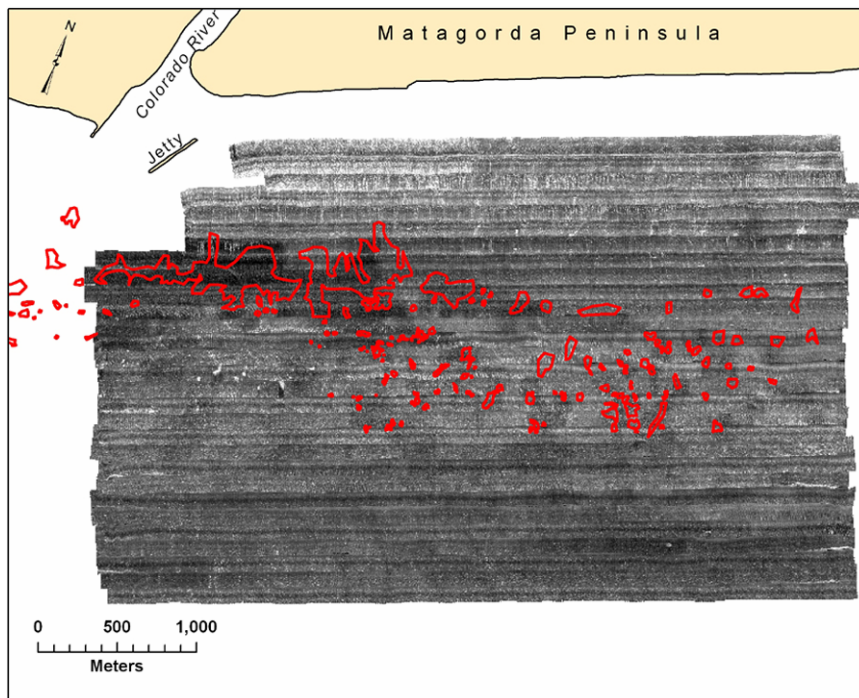


Figure 9: Sidescan sonar mosaic from July 2004. Outlined areas indicate the location of exposed Beaumont Clay found in July 2003.

A comparison of bathymetry data between July 2003 and July 2004 revealed a large loss of sediment from the upper shoreface during the year (Figure 10). In some areas of the upper shoreface, up to 0.4 m of sediment was eroded. Comparison of bathymetry profiles also illustrates this loss of sediment from the upper shoreface and the sediment gain within the scoured area (Figure 11).

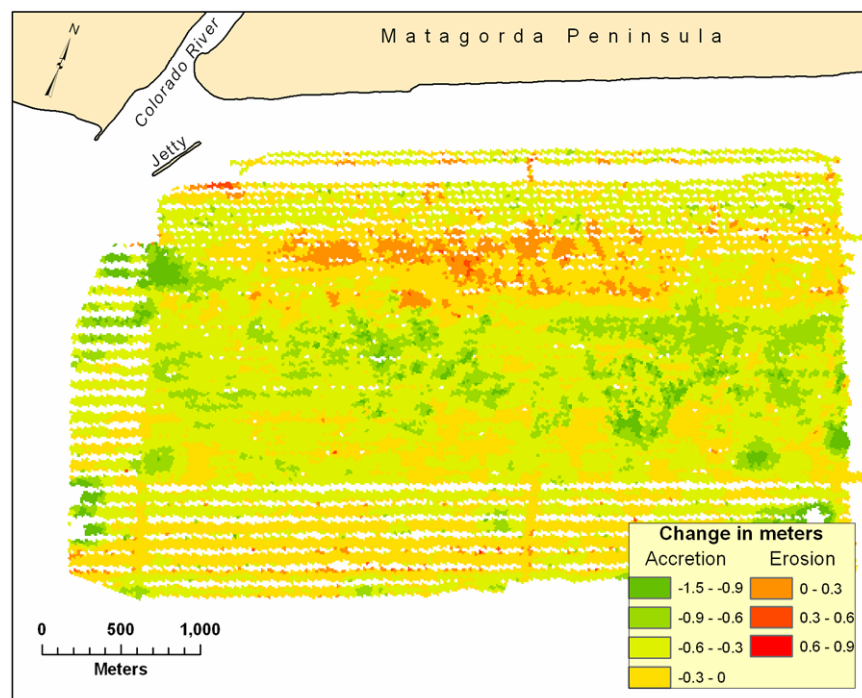


Figure 10: Change in bathymetry between July 2003 and July 2004. Significant erosion of the upper shoreface is notable, along with sediment accretion on the lower shoreface due to the infilling of the scour pits.

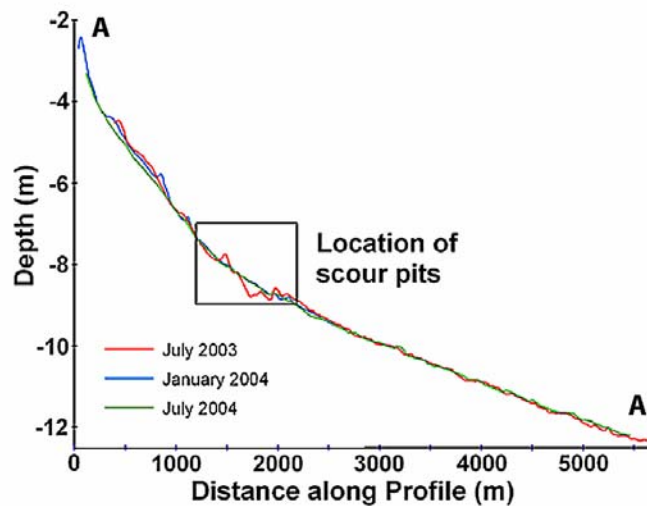


Figure 11: Bathymetric profile measured during each survey. The profiles illustrate the rapid infilling of the scour pits and the loss of sediment from the upper shoreface following the hurricane.

5.2 Seismic Sonar

Chirp seismic sonar data from July 2003 measured the depth of the interfluvial Holocene sediment deposit across the shoreface (Figure 12). The inshore extent of the deposit coincided with the break in shoreface slope, roughly 1 km offshore of the beach in 7 m water depth. Holocene sediment thicknesses within the zone of exposed clay bottom scours ranged from 0.3 to 1.0 m. The sediment layer continued to thicken offshore, reaching a maximum thickness of 2.5 m at a distance of 3 km from the beach. Chirp lines passing directly over the scour pits confirmed that the pits had been eroded completely through the Holocene sediments but had not significantly eroded the Beaumont Clay surface (Figure 13).

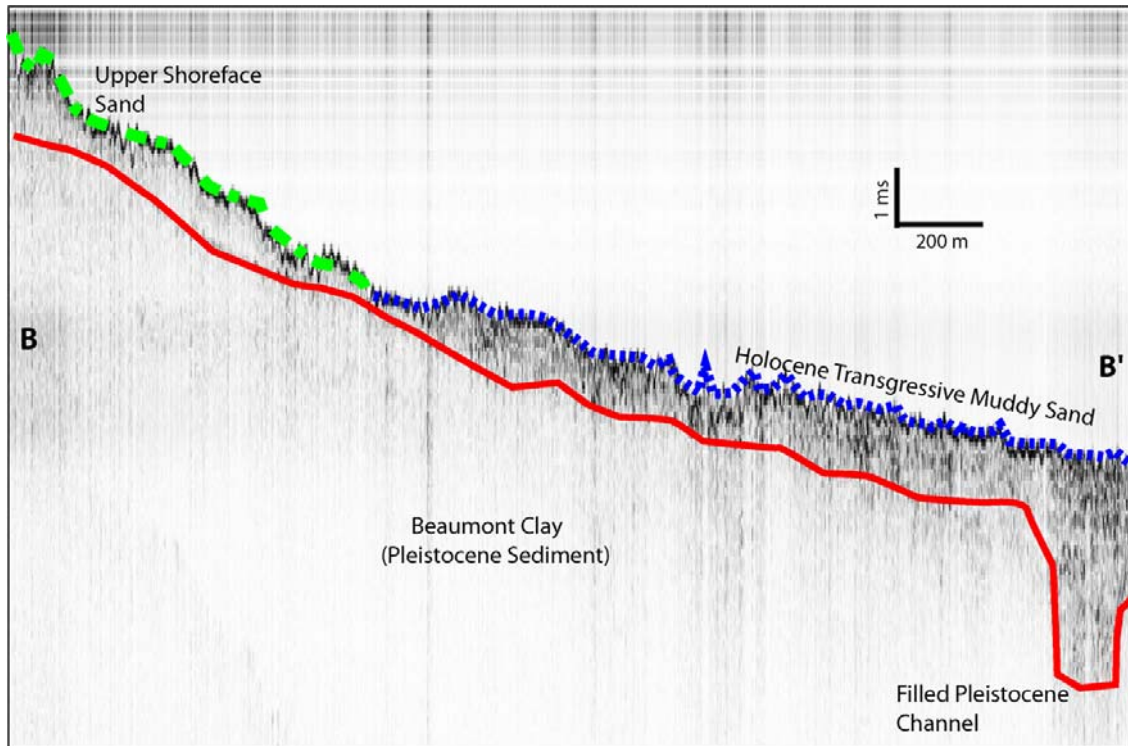


Figure 12: Shore normal Chirp profile showing the stratigraphic surfaces within the shoreface. Proximity of the Beaumont Clay to the seafloor explains the low accommodation space found throughout this stretch of the coast.

Chirp sonar was also used in July 2004 to search for evidence of the scour pits in the stratigraphic record. Multiple passes directly over the sites of former scour pits did not reveal any conclusive evidence of their existence. The sediment filling the pits exhibited an identical seismic signature as the sediment surrounding the pits.

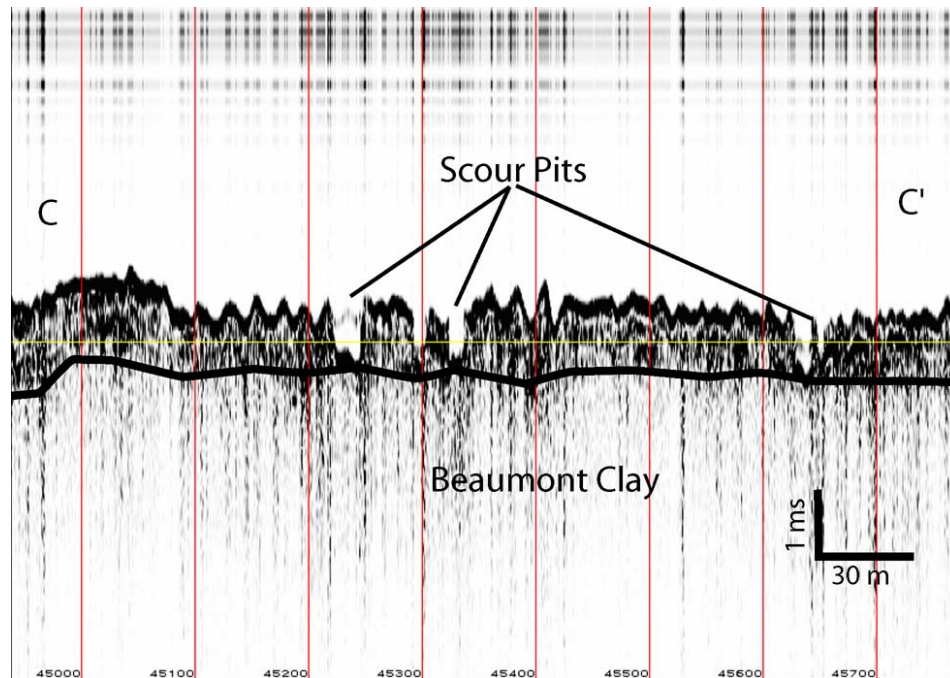


Figure 13: Chirp seismic data across a series of clay floored scour pits on the lower shoreface. The pits have been scoured through the Holocene sediments into the Beaumont Clay surface.

5.3 Surface Sediment Samples

Sediment grain size distribution measured in July 2003 ranged from nearly 100% sand on the upper shoreface to nearly 100% mud within 7 km of the beach (Figure 14). Very fine grained sand (modal size of 0.088 mm) dominated the upper shoreface from the inshore extent of the survey to 7 m water depth. Offshore of this depth the sediment rapidly transitioned to 1:1 ratio of sand to mud. This transition coincided with the break in slope of the shoreface and the exposed clay belt. The sediment became increasingly muddier with distance from shore. Only one exception to the sandy upper shoreface was found. This occurred within 700 m of the beach where the sample contained 75 % mud.

By January 2004, the only noticeable changes to grain size distribution involved

the exception mentioned above (Figure 15). The inshore site was now almost 90 % sand. Elsewhere on the shoreface, the across shore gradient of sand to muddy sand was maintained.

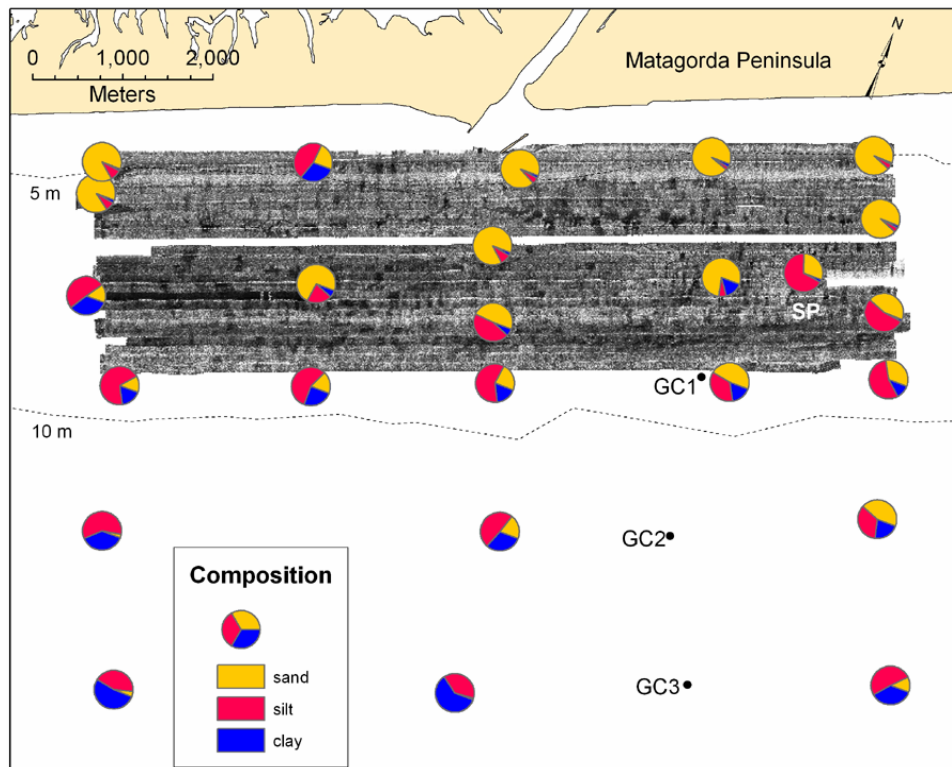


Figure 14: Surface sediment grain size distribution for July 2003 and location of gravity cores (GC). Location of scour pit sample denoted by "SP".

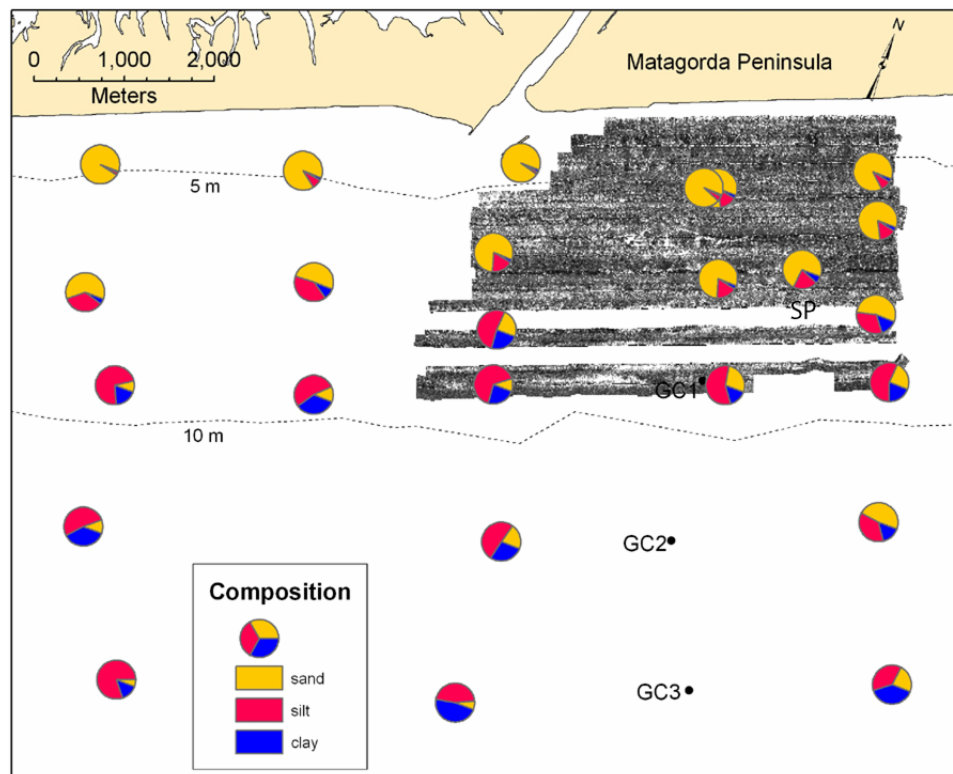


Figure 15: Surface sediment grain size distribution for January 2004 and location of gravity cores (GC). Location of scour pit sample denoted by "SP".

Samples collected in July 2004 showed increased mud content of the inshore samples and increased sand content of the offshore samples (Figure 16). Samples on the upper shoreface, that were previously 90 to 95% sand, were 50 to 75% mud. Offshore samples that were close to 100% mud a year ago had sand contents of 75%.

Repeated grab samples from the location of a large, clay floored pit in 8.2 m water depth tracked the type of sediment infilling this feature (Figures 14 – 16). In July 2003, sediment containing 75% mud was recovered. Stiff orange clay was found on the exterior of the grab sampler. The sample recovered in January 2004 was over 70% sand. There was no clay observed on the grab sampler at this time. The July 2004 sample from

the large scour pit remained close to its January value of 75% sand. Again, there was no evidence of the clay.

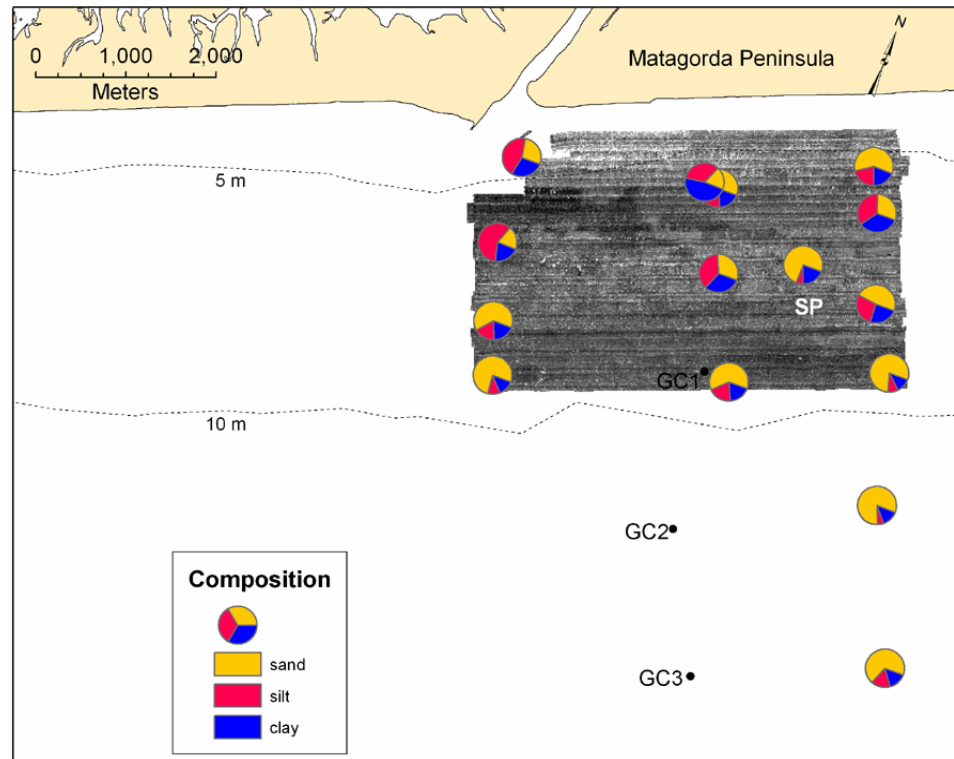


Figure 16: Surface sediment grain size distribution for July 2004 and location of gravity cores (GC). Location of scour pit sample denoted by "SP".

5.4 Sediment Cores

X-ray images of the cores revealed the sedimentary fabric within the Holocene sediment unit (Figure 17). The inshore core (GC1) contained numerous laminations with relatively low bioturbation between 60 cm and the base of the core. This region of the core had a relatively low sand content (Figure 17). Above this layer, a 25 cm thick layer of bioturbated sediment with a high sand content was present. Another muddy layer occurred above the bioturbated sand layer between 25 and 35 cm depth. Again, there was little bioturbation in this layer. Sand content and effects of bioturbation increased towards the top of the core. A layer of transient, fluffy mud occurred in the upper 5 cm of the core. Cores GC2 and GC3 both contained a sandy unit near their base. In GC3, this sandy layer was underlain by mud to the base of the core. Above the deep sand layers both GC2 and GC3 were composed primarily of layers of bioturbated, sandy mud. Some layers exhibited a more laminated appearance.

The base of each core contained a plug of Beaumont Clay. This layer consisted of stiff, orange clay of the Beaumont Clay. The surface of the clay layer varied in depth from 69 to 83 cm. One additional core was attempted from the center of the same large scour pit sampled with the grab sampler. The core tube was recovered empty but the cutting head and outside of the core barrel was covered in stiff, orange clay.

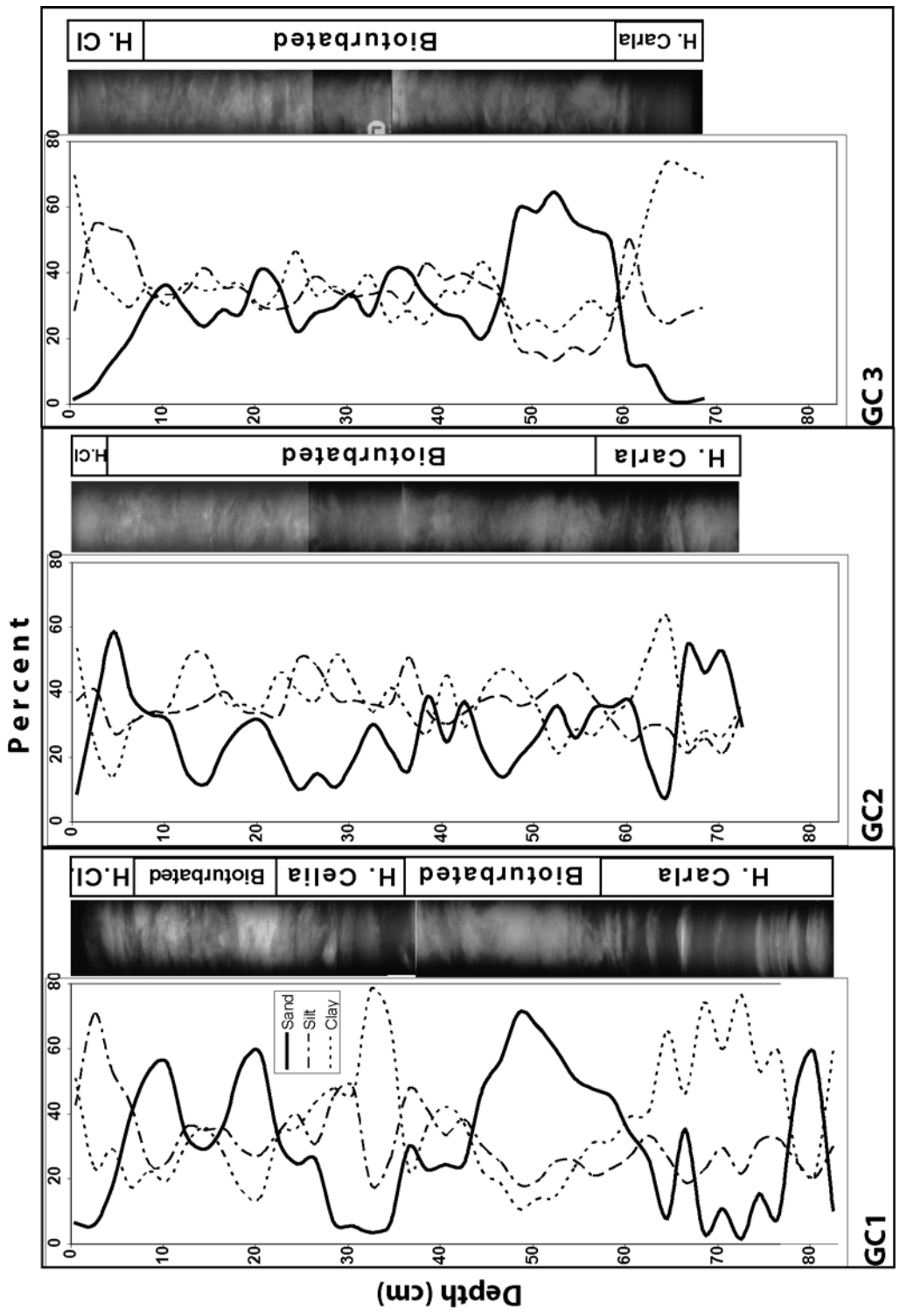


Figure 17: Grain size distribution profiles and x-rays for all three cores. Approximate contributions of Hurricanes Carla, Celia, and Claudette to the sediment record are shown to the right of each x-ray.

5.5 Waves and Combined Flow

The maximum offshore wave heights recorded at NOAA buoy 42019 for Hurricane Claudette were 5.5 m with a period of 10 s. Analysis of breaking location for these offshore waves shows that they would break in 7 m water depth. Adding a 1 m storm surge places the breaking waves near the 6 meter depth contour of the multibeam sonar data. Calculation of U_{*cw} resulted in maximum values of 27.5 cm s^{-1} (Figure 18). This value greatly exceeded the critical shear velocity of 1.7 cm s^{-1} required to mobilize 0.088 mm sand. Individual contributions of U_{*c} and U_{*wm} revealed that the majority of the combined flow was controlled by wave forcing. However, the current forcing contribution still exceeded the U_{*cr} value.

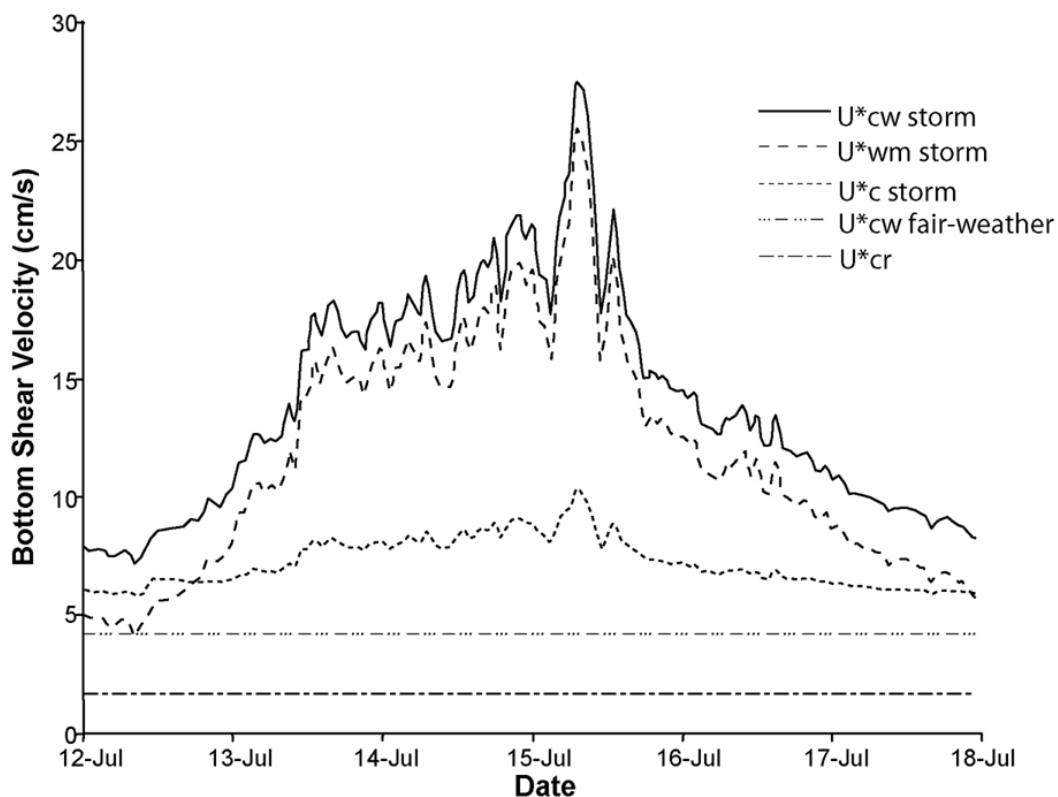


Figure 18: Time-series bottom shear stress velocities calculated for 8 m water depth.

6. DISCUSSION

6.1 Mechanisms for Shoreface Scouring

6.1.1 Waves

Waves erode the seafloor by transferring energy to sediments through oscillating currents as a wave passes overhead. This stirring action is the main force responsible for the initiation of sediment movement across the continental shelf (Madsen, 1993). Calculations of bottom shear stress due to wave action (U_{*wm}) during the landfall of Hurricane Claudette were found to greatly exceed the U_{*cr} values for 0.088 mm sand. Further simulations of U_{*wm} under fair-weather conditions illustrates the intense power of the hurricane waves compared to conditions normally found along the Texas coast (Figure 18).

Wave breaking is the method by which a wave dissipates the majority of its energy (Komar, 1998). The depth range where incoming waves reached their highest values of U_{*wm} and then broke would have been a region of intense bottom stresses and a large amount of erosion would be expected in this area. This area coincided with the region of heavy scouring shown in Figures 3 and 4.

6.1.2 Currents

Although no water current data was collected at the study site during the landfall of Hurricane Claudette, speculation into the type and intensity of currents present during landfall can be made based on existing hurricane literature. During fair-weather conditions, currents play a vital role in the transport of sediment and a secondary role in the mobilization of sediment (Madsen, 1993). However, the intense currents present

during a hurricane would not only be capable of transporting sediment over a great distance, but also have an increased role in the initial mobilization of sediment (Swift et al., 1985).

Two basic arguments exist for the nature of coastal flow during the landfall of a hurricane. The first argument supports downwelling in a layered flow field, and the theory calls for an onshore flow in the upper layer as a result of shore-parallel winds experienced during the approach and landfall of a hurricane (Swift and Niedoroda, 1985 and Snedden et al., 1988). As a result, sea-level setup occurs on the coast and a cross-shelf pressure gradient is formed. The downwelling due to the pressure gradient drives an obliquely offshore oriented bottom current. Snedden et al. (1988) used the layered flow field to describe storm flows along the Texas coast for both tropical storms and hurricanes Allen (1980) and Carla (1961). Similar downwelling flows have been attributed to coastal setup by Hurricane Hugo (Gayes, 1991), a severe northeaster along the northeastern Atlantic coast of the United States (Madsen et al., 1993 and Wright et al., 1994), and large storm events in others areas of North America (Cacchione et al., 1984, Héquette and Hill, 1993; Héquette et al., 2001; Amos et al., 2003).

The second flow field argument supports a single layer, storm surge controlled coastal flow. This method was proposed by Hayes (1967) based on observations of damage from hurricanes Carla (1961) and Cindy (1963) and summarized by McGowen and Scott (1975). The flow field present in the single layer scenario is characterized by strong unidirectional currents onshore during the approach and landfall of the storm, a rapid reversal of current direction, and finally a strong ebb current as the storm surge is released back into the sea. Moreover, ebb flows can be enhanced when they are in close

proximity to barrier breaches (Siringan and Anderson, 1994). Recent work by Allison et al. (in review) offers direct current measurements of the single layer flow associated with Hurricane Lili (2002) on the Louisiana coast. An ADCP equipped buoy located in 5 m water depth recorded single layer onshore flow exceeding 1 m s^{-1} during the approach of the hurricane, and a rapid (1-2 hour period) reversal of current occurred as the hurricane past the buoy.

The single layer flow field is considered most likely to have occurred on the shoreface during the landfall of Hurricane Claudette. This assumption is based on the similarities between Hurricane Claudette and Hurricane Lili. Both storms were fast moving and caused sea-level setup for around 12 hours near the landfall locations. The single-layer flow measurements from Hurricane Lili were made in water depths similar to those found within the Matagorda Peninsula study site. Also, the proximity of a barrier island breach to the study area (Figure 1) supports the single-layer flow argument.

Regardless of the exact mechanism responsible for flow on the shoreface, extreme bottom currents are one characteristic of hurricane impact. Velocity measurements of bottom currents during hurricane landfalls range from 1 m s^{-1} during Hurricane Lili (Allison et al., in review) to 2 m s^{-1} during Tropical Storm Delia (Forristall et al., 1977) to nearly 3 m s^{-1} during Hurricane Carla (Snedden et al., 1988). Average fair-weather bottom velocities measured by Hall (1976) near Galveston, Texas, were 15.4 cm s^{-1} . These severe flows during hurricanes illustrate the ability of currents to transition from their secondary role as sediment mobilizers to a primary force causing shoreface erosion.

6.2 Formation of Shoreface Scours

Scouring of the shoreface would have been initiated during the approach and landfall of Hurricane Claudette. During this period, the seafloor would have been subject to the strongest combined shear velocities of the storm (Figure 18). Both intense wave energy and an onshore bottom flow in excess of 1 m s^{-1} would have caused immense erosion and onshore transport of sediment. This is also the period in which the large breach at Three Mile Lake was formed through Matagorda Peninsula (Figure 1). Numerous smaller washover fans were also formed, especially south of the Colorado River mouth. The breach and washover fans would have provided sinks for the eroded shoreface sediment during the waxing phases of the storm (McGowen and Scott, 1975).

The geologic framework of the shoreface was responsible for different patterns of erosion found there. Areas of sandy sediment exhibited channelized scours oriented parallel to the major onshore and offshore current flow direction. Areas with muddier sediments exhibited rounder, deeper pit-like scours. The most obvious erosional pattern found on the shoreface was the series of large, clay floored pits scoured through the muddy sand (Figures 3, 4, and 6). The varying size of these pits and the seemingly randomness of their individual locations illustrates the complexity of sediment transport fields during hurricanes (Bentley et al., 2002).

Due to their location on the shoreface, these scour pits would have been exposed to some of the highest wave shear velocities. Their position at the base of the shoreface break in slope may also have exposed them to increased current velocities due to constriction of the water column. The intense combined flows would have initiated the scouring of the pits. Once the pit was started, the rough seafloor surface would have

created higher shear stresses. This would create a positive feedback for erosion and allow for the continued excavation of the pit. Deepening of the pits continued until the stiff Beaumont Clay surface was exposed at their bases. Seismic records indicated that the scouring did not continue far into the Pleistocene surface (Figure 13).

Erosion of the scour pits continued into the waning stages of the storm. This was evident by the debris fields stretching in an offshore direction from the pits (Figure 6). These debris fields may have been composed of rip-up clasts from erosion of the Beaumont Clay. As the offshore current weakened during the departure of the storm, the debris fields were deposited along the final direction of the flow.

The belt of Beaumont Clay (Figure 3) that ran along the study site at the base of the break in slope was also exposed during the waxing phase of the storm. The location of this area between the sandy upper shoreface and the marine sediments of the lower shoreface suggested that there was little modern sediment covering the Pleistocene surface before the storm. The clay would have been easily exposed by the intense shear velocities early in the storm. The depth of the scouring in this area was also controlled by the location of the Pleistocene surface. Once this surface had been exposed, little further scouring took place in the stiff Beaumont Clay.

Offshore of the pits floored with Beaumont Clay, another series of pits were formed (Figure 7). The scouring of these pits did not reach the depth of the Pleistocene surface. Their location in deeper water would have led to lower wave shear stresses and their distance from the break in slope may have resulted in decreased bottom flow velocities. These pits also lacked associated debris fields.

Similar pits also occurred throughout the lower shoreface in the southern half of the survey area. A number of explanations may account for the almost total lack of pits with exposed clay bottoms there. First, the southern half of the survey was located up to 5 km closer to the center of the storm. This slight difference in distance may have caused critical differences in wave height and bottom currents along the survey area. This may have resulted in combined flows that simply were not able to scour deep pits.

Second, Hurricane Claudette was a fast moving storm that did not provide a large time window for erosion of the shoreface during its approach. Accordingly, the clay floored pits may have required the extra erosion provided by strong offshore currents during the waning period of the storm for their complete formation. The magnitude of these flows would be greatest in front of barrier island breaches or natural channels that allowed the drainage of the swollen bay waters (Scott and McGowen, 1975). The clay floored pits located in the northern half of the survey area were situated just offshore of the large breach that opened at Three Mile Lake (Figure 1). The only clay floored pits located in the southern half of the survey occurred offshore of the Colorado River Mouth. These two channels would have been the main conduits for receding water between Matagorda Bay and the open Gulf of Mexico.

Finally, the pits may have initially been scoured down to the Pleistocene surface and then partially filled before the survey took place. Three immediate sources of sediment were available for filling the scour pits. The pits were located downstream from the mouth of the Colorado River. Effects of storm surge and flooding due to rainfall, however minor, would have increased the terrestrial sediment supply from the river to the inner shelf following the hurricane. Also, suspended sediment from a

dredging operation taking place at the mouth the river may have also contributed to the supply. The presence of muddy sediments on the upper shoreface found in July 2003 has been attributed to these dredging operations (Figure 14). Finally, sand deposited behind a weir in the northern jetty represented a large potential source of sediment. Some of this sand may have been transported onto the shoreface during the receding storm surge and deposited in the pits.

The channelized scours located on the upper shoreface (Figure 5) were similar in relief and location to features reported by Gayes (1991) following Hurricane Hugo's (1989) landfall on the South Carolina coast. Gayes speculated that these features were formed either by strong offshore bottom currents or by storm intensified rip current cells. However, the features reported by Gayes (1991) and other workers (Cacchione et al., 1984; Thielor et al., 1995; Thielor et al., 2001; Amos et al., 2003) were floored with rippled sand. The channels on the Matagorda shoreface did not display rippled bottoms.

Evidence of former scouring of the shoreface within the study area was provided by the gravity cores collected (Figure 17). Alternating layers of laminated, physically deposited sediments and bioturbated sediments suggest periods of rapid and slow sediment deposition, respectively. The 25 cm thick layer of laminated sediment at the base of GC1 indicates rapid deposition directly on top of the Beaumont Clay surface found at the base of the core. Similar laminated deposits at the bases of GC2 and GC3 also indicate a large deposition event. These deposits may have been formed by Hurricane Carla, a Category 5 hurricane, which made landfall approximately 50 km south of the study area in 1961. This powerful storm may have completely scoured the Holocene sediment from the inner continental shelf and then deposited a storm layer

directly on the Pleistocene surface. The upper portion of that deposit was susceptible to biological disturbance after the storm, resulting in the bioturbated sand layer found above the laminated sand and mud layers. A contact located 35 cm deep in GC1 may represent the depth of erosion due to Hurricane Celia in 1970. Above this contact is a smaller laminated mud layer with bioturbated sands above that. Around 10 cm deep, the sand layers in GC1 become more laminated. This may represent the deposition of a Hurricane Claudette storm layer. The upper 5 cm of the core consisted of a fluffy, transient mud layer.

6.3 Recovery of the Shoreface

In the wake of Hurricane Claudette, the shoreface of Matagorda Peninsula was a heavily eroded surface (Figures 3 and 4). However, within 6 months of the storm the seafloor had transitioned into a relatively smooth and featureless surface (Figure 8). This surface was similar to other Texas shorefaces surveyed during fair-weather periods (Robb et al., 2003, Dellapenna et al., 2001; 2002). The transition from a storm to a fair-weather surface would have required a large input of sediment to reestablish the grade of the shoreface and a transport mechanism capable of moving that sediment into the study area. With a large portion of the eroded shoreface sediment sequestered behind the dunes of Matagorda Peninsula or lost to the inner continental shelf, the shoreface would require a distal sediment source to make its recovery.

The primary sediment supply and driving mechanism for recovery would have been provided by longshore drift. The central Texas coast marks an area of converging longshore drift currents from south and east Texas. This convergence results in a high

sediment supply to the region (Rodriguez et al., 2001). Secondary sediment supplies may have included sediment input from the Colorado River, offshore transport of beach sands deposited on the upper shoreface, and onshore transport of sediment from the continental shelf. The relative lack of bedforms in the sidescan sonar records from all three surveys suggests that bedload transport was not the primary mode of transport for these sediments. Instead, deposition of suspended sediment would have been the primary source of sediment during the recovery.

Due to the depressed relief of the scour pits on the shoreface surface, they created localized areas of relatively high accommodation space. This allowed sediment that normally would bypass the area to accumulate within the scour pits. It was the combination of increased accommodation space and high sediment supply that led to the rapid infilling of the scour pits following the storm. Once the pits had completely filled, sediment would resume bypassing the study area for regions of higher accommodation space. This may explain the increase in the sand content of offshore grab samples taken in July 2004 (Figure 16). As accommodation space higher on the shoreface disappeared with the recovery of the scours, sand deposition may have occurred lower on the shoreface.

The only feature still visible by July 2004 was the outcropped clay belt located at the base of the upper shoreface (Figure 9). This feature was similar in position to the outcrops reported by Robb et al (2003) on the Galveston Island shoreface. The belt occurred in an area where the sediment layer during fair-weather would have been thin compared to the adjacent upper shoreface sand and lower shoreface muddy sand. The presence of this layer in all three sidescan sonar surveys suggested that it was continually

exposed throughout the year. The inability of sediment to accumulate there was due to a total lack of accommodation space above the Beaumont Clay.

6.4 Implications for the Inner Continental Shelf

6.4.1 Transgressive Layer Dynamics

Sediment cores collected on the inner continental shelf near the study site show that the transgressive Holocene strata were composed of numerous storm layers superimposed on one another (Figure 17). These storm beds were similar to those reported by Rodriguez et al (2001) throughout inner shelf sediments of the central Texas coast. Their prevalence in the sediment record suggests that offshore transport of sediment during storms was the primary agent for inner continental shelf deposition.

The strong offshore currents encountered during the waning period of the storm would have transported a large amount of shoreface sediment onto the continental shelf. This sediment would have been deposited as a storm layer on top of the transgressive Holocene sediment. Since the layer was deposited below the depth of ravinement (Swift, 1968), it was unaffected by fair-weather shoreface processes and became preserved as a part of the transgressive unit. Storage of this sediment offshore effectively removed it as a source of sediment for shoreface recovery following the storm.

6.4.2 Implications for "Profile of Equilibrium"

The classic model describing shoreline profile change is the Bruun Rule (Bruun, 1962). This model relies on a set of basic assumptions applied to shorelines throughout the world to determine their "profile of equilibrium". However, Pilkey et al (1993)

presented strong arguments against the use of such blanket assumptions. Together with another critical review by Thielert et al (1995) several points are illustrated with field observations suggest that shoreface geology is much more complex than the assumptions of the Bruun Rule. Further strengthening of the points made by Pilkey et al (1993) and Thielert et al (1995) against these assumptions can be gathered using observations from the Matagorda shoreface after Hurricane Claudette. These assumptions and arguments against them have been summarized into four sections.

The first assumption is that the shoreface is composed of an infinitely thick layer of uniform grain size sand. Grain size analysis of surface grab samples throughout the study area indicated that this was not the case (Figures 14, 15, and 16). Although there was no change in the modal grain size (0.088 mm) of the sand found throughout the study area, the relative contributions of sand and mud changed over an across-shore gradient. The second part of this assumption deals with the thickness of the shoreface sands. Although the upper shoreface contained a relatively thick layer of sand (Rodriguez et al., 2001), the lower shoreface was covered with a thin layer of muddy sand. An exposed belt of basement material stretched between the two zones where there was no sediment cover at all.

The second assumption deals with the ability of underlying geology to affect the shoreface profile. Due to an infinitely thick sand layer the Bruun Rule assumes that there was no underlying geology to control the shoreface profile. On the shoreface of Matagorda Peninsula, the underlying geology was Beaumont Clay, which represents the Pleistocene ravinement surface. Along this interfluvial region, where accommodation space was low due to the proximity of the Beaumont Clay to the surface, the slope of the

lower shoreface was controlled by the underlying geology. Also, the depth of erosion along certain portions of shoreface was controlled by the underlying geology, which inhibited continued profile modification once it had been exposed.

The third assumption was that all sediment movement was caused by waves. Although the wave forcing on the seafloor was intense during the hurricane and a likely cause for the initiation of sediment transport, waves are incapable of transporting sediment great distances due to their oscillating flow (Madsen, 1993). The intense on- and offshore currents during the hurricane would have been able to transport sediment much more efficiently than the waves alone.

The final assumption was that sediment was not exchanged across the depth of closure. This effectively meant that shoreface sediments were never transported offshore to the continental shelf, even during storms. Evidence from sediment cores (Figure 17) showed that sandy storm layers were present on the inner shelf. The mechanism for the formation of these layers requires the current borne shoreface sediments to cross the depth of closure to reach their deposition sites.

6.4.3 Geohazards to Shoreface Development

Geohazard is a term used in the offshore exploration industry to describe any geological risks posed to the development of a production field (Barton, 2003). The scour pits located on the shoreface of Matagorda Peninsula would most certainly pose a risk to any development of the shoreface and can therefore be classified as shallow water geohazards. Standing amongst the field of scour pits were four oil platforms and a series of pipelines. Figure 19 shows the proximity of the scouring to one of the wells.

Although there was no apparent damage to the wells or pipelines, the scour pits would undoubtedly be concerning to the owners of these wells and should be a consideration for anyone interested in shoreface development.

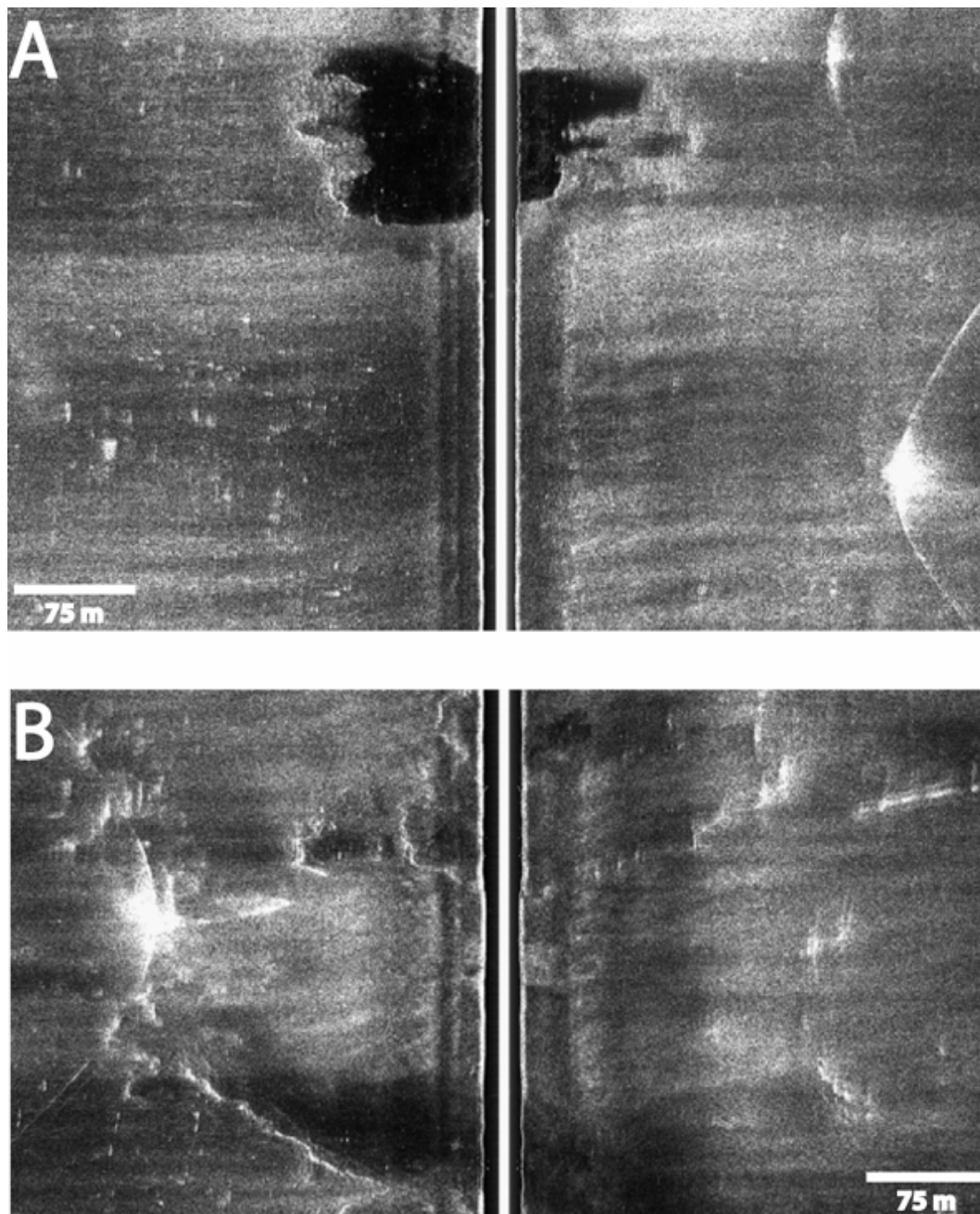


Figure 19: Sidescan sonar images from July 2003. Oil platforms appear at the apex of the hyperbolic features. The scouring in image A is a pit floored with Beaumont Clay. Scouring in image B is a large muddy sand floored pit.

7. CONCLUSIONS

Previous sidescan sonar and bathymetry surveys (Robb et al., 2003, Dellapenna et al., 2001; 2002) have found the fair-weather configuration of the Texas shoreface to be a gently sloping surface with relatively featureless bathymetry. However, following the landfall of Hurricane Claudette, high relief (8 to 103 cm) scours were found on the shoreface of Matagorda Peninsula (Figure 6). Based on the location and timing of these phenomenon, their formation has been attributed to erosion during the hurricane. The processes responsible for scouring the seafloor during the hurricane were intense onshore and offshore currents (with probable magnitudes exceeding 1 m s^{-1}) and extreme bottom shear velocities (27.5 cm s^{-1}) (Figure 18).

The scoured surface was divided into three categories based on the extent of scouring and position on the shoreface. The formation of each type of scour was controlled by a combination of the erosional forces and the geologic framework present in their immediate areas. On the upper shoreface, shore normal channels were formed in the sandy sediment (Figure 5). These channels were produced either by the strong bottom currents present or by storm intensified rip current cells. On the lower shoreface, two types of scour pits were recognized. The first types were pits floored by exposed Beaumont Clay (Figure 6). These pits exhibited the highest relief on the erosional surface and penetrated completely through the thin layer of Holocene marine sediment to the underlying Beaumont Clay surface. The second type of scour pit consisted of lower relief pits that occurred within the Holocene sediment layer (Figure 7). These pits were ubiquitous throughout the lower shoreface, except where the clay floor pits occurred.

Transition of the shoreface from the scoured post-storm surface to a relatively featureless fair-weather surface took place within 6 months of the storm. By January 2004, the scour pits had been filled with muddy sand and the shoreface channels were no longer detectable in sidescan sonar data (Figure 8). Twelve months after the storm, the shoreface still exhibited a featureless fair-weather configuration (Figure 9).

The sediment source most likely responsible for the rapid recovery was from longshore drift. Secondary sources of sediment may have included sediment from the Colorado River and reworking of upper shoreface sediments. Scour pits were rapidly infilled by these sediment sources due to relatively high accommodation space they provided in a region of otherwise low accommodation space.

Erosion of the shoreface during the storm mobilized a large volume of sediment. During the waxing phase of the storm, this sediment was transported by strong onshore currents through breaches and overwashes into Matagorda Bay. Deposition of the sediment would have resulted in a storm layer throughout the inland areas. When the currents reversed direction during the waning phase of the storm, deposition of sediment occurred on the continental shelf. This would have resulted in the formation of a storm layer in the transgressive Holocene strata that covers the continental shelf adjacent to the study site (Figure 17).

Evidence from sediment cores suggested that erosion into or completely through the Holocene transgressive unit may be typical during the approach of a hurricane. During the waning stages of the storm, a layer of highly laminated sediments is deposited. Subsequent, large hurricanes may completely remove this layer and deposit a new layer of their own. Smaller storms may only remove a portion of existing deposits

before laying down deposits of their own. This cycling of erosion and deposition contributes to the low preservation potential of the shoreface.

The complicated pattern of erosion and geologic framework found throughout the study area supports criticism of the concept of shoreface profile of equilibrium and the Bruun Rule (Bruun, 1961) by Pilkey et al (1993) and Thieler et al (1995). Implications for each of the points discussed in the aforementioned papers were illustrated on the Matagorda Peninsula shoreface following the hurricane. These points were the complexity of surface sediment grain size variation and layer thickness, the role of underlying geology as a control on the shoreface profile, transport of sediment by waves and currents, and the cross-shelf transport of sediment onto the inner continental shelf.

Finally, the intensity of the forces present during the hurricane and the heavily eroded surface left behind after the storm represented an immediate threat to structures erected on the shoreface. Due to the depth of scouring in some of the pits, these features not only pose a danger to installations above the seafloor (i.e. wellheads, platforms, and moorings), but also to buried installations such as pipelines. The potential formation of these geohazards on other shorefaces should be of concern to future nearshore development.

REFERENCES

- Abel, C. E., Tracy, B. A., Vincent, C. L., Jensen, R. E., 1989. Hurricane hindcast methodology and wave statistics for Atlantic and Gulf hurricanes from 1956–1975. Wave Information Study Report 19, Waterways Experiment Station, U.S. Army Corps of Engineers, Vicksburg, Mississippi, 85 pp.
- Allison, M. A., Sheremet, A., Goñi, M. A., Stone, G.W., 2005. Storm layer deposition on the Mississippi-Atchafalaya subaqueous delta generated by Hurricane Lili in 2002. Article submitted to *Continental Shelf Research*, in review.
- Amos, C.L., Chiocci, F.L., La Monica, G.B., Cappucci, S., King, E.H., and Corbani, F., 2003. Origin of shore-normal channels from the shoreface of Sable Island, Canada. *Journal of Geophysical Research* 108 (C3), 3094-3110.
- Barton, B. Integration to bring integrity to geohazard investigations. *Offshore Engineer*. 4 Feb. 2003. OilOnline. 19 Apr. 2005 <<http://www.oilonline.com/news/features/oe/20030204.Integrat.10631.asp>>.
- Belknap, D.F., Kraft, J.C., 1981. Preservation potential of transgressive coastal lithosomes on the U.S. Atlantic shelf. *Marine Geology* 42, 429-442.
- Belknap, D.F., Kraft, J.C., 1985. Influence of antecedent geology on stratigraphic preservation potential and evolution of Delaware's barrier systems. *Marine Geology* 63, 235-262.
- Bentley, S.J., Keen, T.R., Blain, C.A., Vaughan, W.C., 2002. The origin and preservation of a major hurricane event bed in the northern Gulf of Mexico: Hurricane Camille, 1969. *Marine Geology* 186, 423-446.

- Bernard, H.A., Major, C.F., Jr., Parrot, B.S., Leblanc, R.J. 1970. Recent sediments of southeast Texas: a field guide to the Brazos alluvial and deltaic plains and the Galveston barrier island complex: The University of Texas at Austin, Bureau of Economic Geology, Guidebook 11, 132 pp.
- Beven, J. 2003. Tropical cyclone report Hurricane Claudette 8-17 July, 2003. NOAA/National Weather Service, Miami, 16 pp.
- Bruun, P., 1962. Sea-level rise as a cause of storm erosion. Proceedings of the American Society of Civil Engineers Journal of Waterways and Harbors Division 88, 117-130.
- Cacchione, D.A., Drake, D.E., Grant, W.D., Tate, G.B., 1984. Rippled scour depressions on the inner continental shelf off central California. Journal of Sedimentary Petrology 54, 1280-1291.
- Dellapenna, T.M., Allison, M., Seitz, W., 2001. Sand resources and movement off Galveston beaches. Final Report to Texas General Land Office. 36 pp.
- Dellapenna, T.M., Allison, M., Seitz, W., 2002. Sand resources and movement off Surfside Beach: Final Report 2000-2002. Final Report to Texas General Land Office. 18 pp.
- Folk, R.L., 1954. The distinction between grain size and mineral composition in sedimentary-rock nomenclature. The Journal of Geology 62, 344-359.
- Forristall, G.Z., Hamilton, R.C., Cardone, V.J., 1977. Continental shelf currents in tropical storm Delia: observations and theory. Journal of Physical Oceanography 7, 532-546.

- Gayes, P.T., 1991. Post-Hurricane Hugo nearshore side scan sonar survey; Myrtle Beach to Folly Beach, South Carolina. *Journal of Coastal Research*, Special Issue 8, 95-111.
- Gibbs, R.J., Matthews, M.D., Link, D.A., 1971. The relationship between sphere size and settling velocity. *Journal of Sedimentary Petrology* 41, 7-18.
- Gibeaut, J.C., White, W.A., Hepner, T., Gutierrez, R., Tremblay, T.A., Smyth, R., Andrews, J., 2000. Texas shoreline change project: Gulf of Mexico shoreline change from the Brazos River to Pass Cavallo, The University of Texas at Austin, Bureau of Economic Geology. 34 pp.
- Hall, G.L., 1976. Sediment transport processes in the nearshore waters adjacent to Galveston Island and Bolivar Peninsula. Ph.D. Dissertation, Texas A&M University, College Station, Texas. 305 pp.
- Hayes, M.O., 1967. Hurricanes as Geological Agents: case studies of Hurricanes Carla, 1961, and Cindy, 1963. The University of Texas at Austin, Bureau of Economic Geology Report on Investigations No. 61, 56 pp.
- Hayes, M.O., 1979. Barrier island morphology as a function of tidal and wave regime. In: Leatherman, S.P. (Ed.), *Barrier Islands from the Gulf of St. Lawrence to the Gulf of Mexico*. Academic Press, New York, pp. 1-28.
- Héquette, A., Desrosiers, M., Hill, P.R., Forbes, D.L., 2001. The influence of coastal morphology on shoreface sediment transport under storm-combined flows, Canadian Beaufort Sea. *Journal of Coastal Research* 17, 507-516.

- Héquette, A., Hill, P.R., 1993. Storm-generated currents and offshore sediment transport on a sandy shoreface, Tibjak Beach, Canadian Beaufort Sea. *Marine Geology*, 113, 283-304.
- Hubertz, J.M., Brooks, R.M., 1989. Gulf of Mexico hindcast wave information. Wave information studies of U.S. coastlines, WIS Report 18, Department of the Army, Corps of Engineers, Waterways Experiment Station, Vicksburg, Mississippi.
- Komar, P.D., 1998. *Beach Processes and Sedimentation: Second Edition*. Prentice Hall, Upper Saddle River, New Jersey. 544 pp.
- Madsen, O.S., 1993. *Sediment Transport on the Shelf*. Massachusetts Institute of Technology, Cambridge, Massachusetts, 143 p.
- Madsen, O.S., Wright, L.D., Boon, J.D., Chisholm, T.A., 1993. Wind stress, bed roughness and sediment suspension on the inner shelf during an extreme storm event. *Continental Shelf Research* 13, 1303-1324.
- McGowen, J.H., Scott, A.J., 1975. Hurricanes as geologic agents on the Texas Coast. In: Cronin, L.E. (Ed.), *Estuarine Research*. Academic Press, New York. pp. 23-46
- National Data Buoy Center, 2003. National Oceanic and Atmospheric Administration. 20 Nov. 2003 <<http://www.ndbc.noaa.gov>>.
- National Ocean Service, 2003. National Oceanic and Atmospheric Administration. 20 Nov. 2003 <http://tidesandcurrents.noaa.gov/data_res.html>.
- Niedorada, A.W., Swift, D.J.P., Figueiredo, A.G., Freeland, G.L., 1985. Barrier island evolution, middle Atlantic shelf, U.S.A. Part II: Evidence from the shelf floor. *Marine Geology* 63, 363-396.

- Pilkey, O.H., Young, R.S., Riggs, S.R., Smith, A.W.S., Wu, H., Pilkey, W.D., 1993. The concept of shoreface profile of equilibrium: a critical review. *Journal of Coastal Research* 9, 255-278.
- Robb, B.K., Allison, M.A., Dellapenna, T.M., 2003. Anthropogenic and natural controls on shoreface evolution along Galveston Island, Texas. *Proceedings of the International Conference on Coastal Sediments 2003*. CD-ROM Published by World Scientific Publishing Corp. and East Meets West Productions, Corpus Christi, Texas, USA. ISBN 981-238-422-7, 13p.
- Rodriguez, A.B., Anderson, J.B., Fernando, P.S., Taviani, M., 2004. Holocene evolution of the east Texas coast and inner continental shelf: along-strike variability in coastal retreat rates. *Journal of Sedimentary Research* 74, 405-421.
- Rodriguez, A.B., Fassell, M.L., Anderson, J.B., 2001. Variations in shoreface progradation and ravinement along the Texas coast, Gulf of Mexico. *Sedimentology* 48, 837-853.
- Schwarzer, K., Diesing, M., Larson, M., Niedermeyer, R.-O., Schumacher, W., Furmanczyk, K. 2003. Coastline evolution at different time scales – examples from the Pomeranian Bight, southern Baltic Sea. *Marine Geology* 194, 79-101.
- Siringan, F.P., Anderson, J.B., 1994. Modern shoreface and inner-shelf storm deposits off the east Texas coast, Gulf of Mexico. *Journal of Sedimentary Research*, B64, 99-110.
- Snedden, J.W., Nummedal, D., Amos, A.F., 1988. Storm- and fair-weather combined flow on the central Texas continental shelf. *Journal of Sedimentary Petrology* 58, 580-595.

- Styles, R., Glenn, S.M., 2000. Modeling stratified wave and current bottom boundary layers on the continental shelf. *Journal of Geophysical Research-Oceans* 105,119-139.
- Swift, D.J.P., 1968. Coastal erosion and transgressive stratigraphy. *Journal of Geology*, 14, 1-43.
- Swift, D.J.P., Niedoroda, A.W., 1985. Fluid and sediment dynamics on continental shelves. In Tillman, R.W., Swift, D.J.P., Walker, R.G. (Eds.), *Shelf Sands and Sandstone Reservoirs*. Soc. Econ. Paleontologists Mineralogists Short Course Notes, no. 13, pp. 47-133.
- Swift, D.J.P., Niedoroda, A.W., Vincent, C.E., Hopkins, T.S., 1985. Barrier island evolution, middle Atlantic shelf, U.S.A. Part I: shoreface dynamics. *Marine Geology* 63, 331-361.
- Thieler, E.R., Brill, A.L., Cleary, W.J., Hobbs III, C.H., Gammisch, R.A., 1995. Geology of the Wrightsville Beach, North Carolina shoreface: implications for the concept of shoreface profile of equilibrium. *Marine Geology* 126, 271-287.
- Thieler, E.R., Pilkey, O.H., Cleary, W.J., Schwab, W.C., 2001. Modern sedimentation on the shoreface and inner continental shelf at Wrightsville Beach, North Carolina, U.S.A. *Journal of Sedimentary Research* 71, 958-970.
- U.S. Army, 1984. *Shore Protection Manual*, 4th ed., 1 Vol., U.S. Army Engineer Waterways Experiment Station, U.S. Government Printing Office, Washington, D.C.
- Wright, L.D., 1995. *Morphodynamics of Inner Continental Shelve*. CRC Press, Boca Raton, FL. 241 pp.

Wright, L.D., Xu, J.P., Madsen, O.S., 1994. Across-shelf benthic transports on the inner shelf of the Middle Atlantic Bight during the "Halloween Storm" of 1991. *Marine Geology* 118, 61-77.

APPENDIX A

CLAY FLOORED SCOUR PIT DATA

Scour Pit Central Position			
Easting (m)	Northing (m)	Area (m ²)	Depth (cm)
211849.2	3166459.2	1993.4	79
211911.4	3166441.5	813.7	61
211972.4	3166420.2	1503.9	63
211980.8	3166463.7	360.7	51
212158.9	3166485.2	1606.9	23
211937.6	3166270.0	1199.1	78
211781.9	3166231.5	179.1	71
211787.2	3166202.3	507.6	79
212104.5	3166491.2	820.3	29
212383.9	3166467.6	675.5	66
212312.3	3166238.8	838.5	50
212075.3	3166132.4	798.2	80
211981.8	3166110.6	308.1	79
211851.7	3165845.5	1150.9	46
212454.3	3166079.1	2390.0	47
211474.5	3165916.0	846.2	64
211288.8	3165860.9	215.1	48
211289.1	3165821.0	2373.6	54
211370.9	3165691.0	1690.4	46
211066.1	3165746.7	5325.3	34
210938.3	3165715.5	139.4	35
210909.6	3165723.3	327.5	36
210698.0	3165805.2	1839.2	97
210807.7	3165944.0	2913.4	98
210397.2	3166094.7	838.6	53
210503.9	3165960.0	983.0	72
210394.9	3165898.8	484.7	88
210422.9	3165895.1	112.5	87
210455.9	3165905.9	77.9	76
210461.5	3165927.8	62.1	52
210519.6	3165930.3	103.6	85
210503.4	3165909.5	60.3	70
210334.2	3165872.1	151.8	58
210333.2	3165827.1	156.7	39
210351.5	3165828.9	56.0	41
210383.5	3165872.7	88.1	84
210535.1	3165955.5	233.3	62
210198.6	3166070.1	7624.5	73
210179.5	3165732.6	126.1	30
210195.5	3165749.4	34.5	11

Scour Pit Central Position			
Easting (m)	Northing (m)	Area (m ²)	Depth (cm)
210277.8	3165821.2	554.9	45
210302.6	3165779.7	8.6	41
210308.8	3165776.8	16.8	41
210307.8	3165770.5	4.7	41
210328.4	3165753.3	19.6	41
210332.6	3165717.7	119.7	12
210221.4	3165735.6	18.0	13
210522.7	3165749.1	428.7	73
210428.9	3165663.9	698.6	86
210597.9	3165596.2	156.0	24
210614.8	3165600.8	15.5	24
210619.4	3165589.1	4.8	24
210618.0	3165539.9	1289.6	47
210694.3	3165541.8	660.3	68
210724.4	3165656.3	427.1	27
210372.6	3165497.5	18.4	31
210279.1	3165441.4	441.6	68
210297.4	3165387.0	386.5	60
210243.8	3165437.4	27.8	68
210389.3	3165279.5	388.9	47
210586.4	3165387.1	313.6	57
210532.5	3165375.7	484.5	48
210527.0	3165351.6	129.8	48
210508.9	3165345.5	35.4	48
210517.8	3165328.6	66.2	48
210509.2	3165318.9	68.5	48
210535.3	3165332.3	90.3	48
210396.2	3165264.0	45.6	47
210407.3	3165295.6	16.3	47
210105.7	3165396.7	260.7	43
209869.3	3165665.0	102.6	52
209930.7	3165657.3	46.9	42
209945.3	3165750.0	420.3	55
209990.1	3165768.3	297.9	63
210160.6	3165835.0	1550.5	70
210116.9	3166008.4	2559.6	22
210851.9	3165810.6	847.0	90
210854.2	3165886.3	884.4	69
210891.7	3165884.5	106.3	68
210892.4	3165822.0	81.8	72
210557.7	3166004.2	916.0	54
211360.9	3165643.2	386.7	43
211426.7	3165704.5	268.7	54
211701.8	3166058.5	1227.9	59

Scour Pit Central Position			
Easting (m)	Northing (m)	Area (m ²)	Depth (cm)
211541.3	3166172.4	2048.1	45
211846.3	3166143.3	133.2	44
211857.0	3166120.2	189.3	69
211772.9	3166041.2	257.0	70
211584.9	3166116.4	116.8	56
211420.6	3165917.0	210.3	26
211575.7	3165949.9	1282.8	38
209904.9	3165816.2	267.5	19
210391.8	3165611.7	968.5	29
210513.3	3165765.1	605.2	73
210013.5	3165913.7	1317.9	8
210482.8	3165941.0	584.2	72
210822.1	3165722.7	550.3	36
212084.7	3166011.2	5665.2	65
212126.0	3165957.3	398.4	68
212115.3	3166250.3	1948.8	80
211755.3	3166318.5	590.0	68
211987.7	3165874.3	125.0	65
211883.7	3166293.6	2020.0	79
211643.7	3166170.2	598.2	91
211737.8	3166239.3	657.8	75
212239.9	3166440.7	1716.3	59
210270.3	3165755.0	2303.9	20
211293.7	3166054.9	9370.0	39
212441.7	3166374.7	2527.1	78
212673.3	3166474.2	750.1	50
211957.0	3165907.7	2971.7	66
211849.9	3166035.6	1066.8	81
211899.7	3166072.7	558.1	76
211777.5	3165982.0	908.3	90
211810.9	3166045.6	787.7	30
211906.2	3165977.1	4601.0	103
211795.8	3165925.8	4114.0	86
210501.3	3166192.5	563.4	17
209473.3	3165785.9	1157.9	46
209489.9	3165713.8	595.2	20
209533.3	3165749.2	468.9	26
209581.8	3165762.4	378.3	32
211405.7	3166210.8	5387.9	21
212258.6	3166613.3	4390.3	34
212606.5	3166720.6	3380.8	46
212815.8	3166839.3	2871.6	37
212517.7	3166502.6	524.0	29

Scour Pit Central Position

<u>Easting (m)</u>	<u>Northing (m)</u>	<u>Area (m²)</u>	<u>Depth (cm)</u>
212380.2	3166639.2	2338.7	39
210803.4	3166207.7	3492.3	69
211471.0	3165786.0	725.4	80
211522.4	3165795.8	372.4	74

APPENDIX B

SEDIMENT GRAIN SIZE

July 2003

Site	Lat. (°)	Long. (°)	%Sand	%Silt	%Clay
1	28.555	-96.010	13.9	69.1	16.9
2	28.541	-96.005	2.9	59.5	37.6
3	28.526	-95.997	4.3	42.8	52.9
4	28.562	-96.017	15.7	50.4	33.9
5	28.572	-96.021	90.0	7.8	2.3
6	28.575	-96.021	88.8	9.4	1.9
7	28.583	-95.999	23.8	46.1	30.1
8	28.572	-95.994	73.0	20.8	6.2
9	28.562	-95.990	18.6	56.6	24.8
10	28.590	-95.977	92.7	5.2	2.2
11	28.582	-95.977	88.5	8.9	2.5
12	28.575	-95.974	48.6	45.2	6.2
13	28.569	-95.971	23.1	59.4	17.5
14	28.556	-95.964	20.2	49.2	30.6
15	28.539	-95.961	1.4	38.8	59.8
16	28.556	-95.916	13.0	50.8	36.2
17	28.571	-95.925	44.3	34.6	21.2
18	28.585	-95.930	33.1	55.4	11.4
19	28.591	-95.933	44.1	54.1	1.8
20	28.599	-95.937	94.1	3.7	2.2
21	28.605	-95.941	94.0	4.5	1.5
22	28.599	-95.958	94.5	2.9	2.6
23	28.588	-95.952	78.7	6.3	15.0
24	28.578	-95.946	47.4	36.0	16.7
25	28.591	-95.943	30.2	67.5	2.3

January 2004

Site	Lat. (°)	Long. (°)	%Sand	%Silt	%Clay
1	28.562	-95.956	83.1	14.1	2.8
2	28.592	-95.944	73.6	20.3	6.1
3	28.578	-95.947	27.9	57.4	14.8
4	28.588	-95.952	79.8	17.3	2.9
5	28.596	-95.958	94.3	4.3	1.5
6	28.604	-95.941	88.2	9.2	2.7
7	28.599	-95.938	82.7	14.1	3.3
8	28.590	-95.934	54.1	31.8	14.1
9	28.585	-95.930	24.1	56.7	19.2
10	28.571	-95.925	48.1	36.5	15.4
11	28.557	-95.916	23.3	37.5	39.2
12	28.539	-95.961	7.2	45.9	46.9
13	28.555	-95.963	20.9	50.8	28.3
14	28.569	-95.971	10.8	65.8	23.4
15	28.575	-95.973	24.3	52.2	23.6
16	28.582	-95.977	79.6	17.7	2.7
17	28.591	-95.978	95.9	2.0	2.2
18	28.562	-95.989	12.6	53.1	34.4
19	28.572	-95.994	50.8	40.0	9.2
20	28.582	-96.000	89.7	8.1	2.2
21	28.575	-96.022	96.6	2.2	1.3
22	28.562	-96.018	61.2	34.4	4.4
23	28.528	-95.998	5.9	80.4	13.7
24	28.541	-96.008	11.5	51.8	36.7
25	28.555	-96.011	9.5	72.5	17.9

July 2004

Site	Lat. (°)	Long. (°)	%Sand	%Silt	%Clay
1	28.592	-95.944	74.7	6.0	19.2
2	28.603	-95.941	59.5	21.2	19.4
3	28.599	-95.938	30.4	35.3	34.3
4	28.591	-95.934	48.3	27.7	23.9
5	28.585	-95.930	79.6	8.7	11.7
6	28.572	-95.925	81.3	4.9	13.7
7	28.557	-95.917	69.3	15.8	15.0
8	28.578	-95.946	62.6	19.4	18.0
9	28.588	-95.952	31.7	37.5	30.8
10	28.596	-95.956	59.9	21.9	18.2
11	28.596	-95.958	19.0	33.5	47.5
14	28.591	-95.978	27.9	44.3	27.8
15	28.582	-95.977	19.7	59.3	21.0
16	28.574	-95.974	64.1	17.6	18.4
17	28.569	-95.971	76.8	10.1	13.1

APPENDIX C

BOTTOM SHEAR VELOCITY

Onshore current velocity = 100 cm s^{-1} at 65 cm above seabed

U_{*cw} Fair-weather = 4.2 cm s^{-1}

U_{*cr} for 0.088 mm sand = 1.7 cm s^{-1}

U_* storm values in cm s^{-1}

Date	Time	Wave Height (m)	Wave Period (s)	U_{*cw}	Storm Values U_{*wm}	U_{*c}
7/12/03	0:00	0.61	7.69	7.9	5.0	6.1
7/12/03	1:00	0.64	6.67	7.8	4.9	6.0
7/12/03	3:00	0.61	7.14	7.8	4.9	6.0
7/12/03	4:00	0.61	5.88	7.5	4.6	5.9
7/12/03	5:00	0.58	5.88	7.4	4.5	5.9
7/12/03	6:00	0.6	6.25	7.6	4.7	6.0
7/12/03	7:00	0.58	7.14	7.7	4.8	6.1
7/12/03	8:00	0.56	5.26	7.2	4.2	5.9
7/12/03	9:00	0.6	5.26	7.3	4.3	5.9
7/12/03	10:00	0.6	6.67	7.7	4.8	6.0
7/12/03	11:00	0.58	12.5	8.4	5.2	6.5
7/12/03	12:00	0.67	12.5	8.6	5.6	6.5
7/12/03	13:00	0.7	12.5	8.6	5.7	6.5
7/12/03	14:00	0.71	12.5	8.7	5.7	6.5
7/12/03	15:00	0.73	12.5	8.7	5.8	6.5
7/12/03	16:00	0.74	12.5	8.7	5.8	6.5
7/12/03	17:00	0.9	11.11	9.0	6.4	6.4
7/12/03	18:00	0.87	11.11	9.0	6.3	6.4
7/12/03	19:00	0.95	11.11	9.2	6.6	6.4
7/12/03	20:00	1.18	11.11	9.8	7.4	6.5
7/12/03	21:00	1.17	11.11	9.8	7.3	6.5
7/12/03	22:00	1.12	10	9.5	7.1	6.4
7/12/03	23:00	1.32	10	10.1	7.7	6.5
7/13/03	0:00	1.44	10	10.4	8.2	6.5
7/13/03	1:00	1.78	10	11.5	9.3	6.7
7/13/03	2:00	1.8	10	11.5	9.4	6.7
7/13/03	3:00	2.03	11.11	12.4	10.2	6.9
7/13/03	4:00	2.15	10	12.6	10.6	6.9
7/13/03	5:00	2.03	10	12.2	10.2	6.8
7/13/03	6:00	2.12	10	12.5	10.5	6.9
7/13/03	7:00	2.04	10	12.3	10.2	6.8
7/13/03	8:00	2.15	10	12.6	10.6	6.9
7/13/03	9:00	2.53	10	14.0	11.9	7.2
7/13/03	10:00	2.32	10	13.2	11.2	7.0
7/13/03	11:00	3.1	10	16.1	14.2	7.7

Date	Time	Wave	Wave	Storm Values		
		Height (m)	Period (s)	U*cw	U*wm	U*c
7/13/03	12:00	3.08	11.11	16.1	14.2	7.8
7/13/03	13:00	3.48	11.11	17.8	15.8	8.2
7/13/03	14:00	3.25	11.11	16.8	14.8	7.9
7/13/03	15:00	3.45	11.11	17.7	15.7	8.1
7/13/03	16:00	3.61	11.11	18.3	16.3	8.3
7/13/03	17:00	3.42	11.11	17.5	15.5	8.1
7/13/03	18:00	3.22	11.11	16.7	14.7	7.9
7/13/03	19:00	3.31	10	17.0	15.0	7.9
7/13/03	20:00	3.32	10	17.0	15.1	7.9
7/13/03	21:00	3.13	10	16.2	14.3	7.7
7/13/03	22:00	3.39	11.11	17.4	15.4	8.1
7/13/03	23:00	3.51	10	17.8	15.9	8.1
7/14/03	0:00	3.6	10	18.2	16.2	8.2
7/14/03	1:00	3.14	11.11	16.4	14.4	7.8
7/14/03	2:00	3.39	10	17.3	15.4	8.0
7/14/03	3:00	3.42	11.11	17.5	15.5	8.1
7/14/03	4:00	3.67	11.11	18.6	16.6	8.3
7/14/03	5:00	3.53	11.11	18.0	16.0	8.2
7/14/03	6:00	3.46	11.11	17.7	15.7	8.1
7/14/03	7:00	3.85	11.11	19.4	17.4	8.5
7/14/03	8:00	3.43	11.11	17.6	15.6	8.1
7/14/03	9:00	3.24	10	16.7	14.7	7.8
7/14/03	10:00	3.2	11.11	16.6	14.6	7.9
7/14/03	11:00	3.23	11.11	16.7	14.8	7.9
7/14/03	12:00	3.7	11.11	18.7	16.7	8.4
7/14/03	13:00	3.9	11.11	19.6	17.6	8.6
7/14/03	14:00	3.57	11.11	18.2	16.2	8.2
7/14/03	15:00	3.81	11.11	19.2	17.2	8.5
7/14/03	16:00	3.99	11.11	20.0	18.0	8.7
7/14/03	17:00	3.93	11.11	19.7	17.7	8.6
7/14/03	18:00	4.17	11.11	20.8	18.8	8.9
7/14/03	19:00	3.58	11.11	18.2	16.2	8.3
7/14/03	20:00	4.19	11.11	20.9	18.9	8.9
7/14/03	21:00	4.33	11.11	21.5	19.6	9.0
7/14/03	22:00	4.4	11.11	21.9	19.9	9.1
7/14/03	23:00	4.17	11.11	20.8	18.8	8.9
7/15/03	0:00	4.34	10	21.5	19.6	8.9
7/15/03	1:00	3.88	10	19.4	17.5	8.5
7/15/03	2:00	3.83	10	19.2	17.3	8.4
7/15/03	3:00	3.51	10	17.8	15.9	8.1
7/15/03	4:00	4.24	10	21.1	19.1	8.8
7/15/03	5:00	4.6	11.11	22.8	20.8	9.3
7/15/03	6:00	4.84	10	23.9	22.0	9.5
7/15/03	7:00	5.55	10	27.5	25.5	10.3

Date	Time	Wave	Wave	Storm Values		
		Height (m)	Period (s)	U*cw	U*wm	U*c
7/15/03	8:00	5.5	9.09	27.1	25.1	10.1
7/15/03	9:00	5.24	8.33	25.5	23.5	9.7
7/15/03	10:00	4.42	8.33	21.5	19.6	8.8
7/15/03	11:00	3.66	7.69	17.8	15.9	7.9
7/15/03	12:00	4.19	7.14	19.6	17.8	8.3
7/15/03	13:00	4.56	8.33	22.1	20.3	8.9
7/15/03	14:00	3.94	8.33	19.3	17.4	8.3
7/15/03	15:00	3.51	9.09	17.6	15.7	8.0
7/15/03	16:00	3.49	8.33	17.3	15.5	7.9
7/15/03	17:00	3.29	8.33	16.5	14.6	7.7
7/15/03	18:00	2.81	10	15.0	13.0	7.4
7/15/03	19:00	3	8.33	15.4	13.4	7.4
7/15/03	20:00	2.92	8.33	15.0	13.1	7.3
7/15/03	21:00	3.01	7.69	15.1	13.3	7.3
7/15/03	22:00	2.85	7.69	14.5	12.6	7.2
7/15/03	23:00	2.76	8.33	14.4	12.5	7.2
7/16/03	0:00	2.73	9.09	14.5	12.6	7.3
7/16/03	1:00	2.74	7.69	14.1	12.2	7.1
7/16/03	2:00	2.75	8.33	14.4	12.5	7.2
7/16/03	3:00	2.46	7.69	13.1	11.2	6.9
7/16/03	3:59	2.35	8.33	13.0	11.0	6.9
7/16/03	4:59	2.37	7.69	12.8	10.9	6.8
7/16/03	5:59	2.38	7.14	12.6	10.7	6.7
7/16/03	6:59	2.53	7.69	13.4	11.5	6.9
7/16/03	7:59	2.48	7.69	13.2	11.3	6.9
7/16/03	8:59	2.62	7.69	13.7	11.8	7.0
7/16/03	9:59	2.72	7.14	13.8	11.9	7.0
7/16/03	10:59	2.43	7.14	12.8	10.9	6.8
7/16/03	11:59	2.65	7.14	13.5	11.6	6.9
7/16/03	12:59	2.33	6.67	12.2	10.2	6.6
7/16/03	13:59	2.25	7.14	12.2	10.2	6.6
7/16/03	14:59	2.55	7.69	13.5	11.5	6.9
7/16/03	15:59	2.29	6.67	12.1	10.1	6.6
7/16/03	16:59	2.18	7.14	12.0	10.0	6.6
7/16/03	17:59	2.09	7.14	11.7	9.7	6.5
7/16/03	18:59	2.09	7.14	11.7	9.7	6.5
7/16/03	19:59	2.08	7.69	11.9	9.9	6.6
7/16/03	20:59	1.88	7.69	11.3	9.2	6.5
7/16/03	21:59	1.88	7.14	11.1	9.0	6.4
7/16/03	22:59	1.97	7.14	11.3	9.3	6.5
7/16/03	23:59	1.78	7.14	10.8	8.7	6.4
7/17/03	0:59	1.83	7.14	10.9	8.9	6.4
7/17/03	1:59	1.73	7.14	10.6	8.5	6.3
7/17/03	2:59	1.54	7.14	10.1	8.0	6.2

Date	Time	Wave	Wave	Storm Values		
		Height (m)	Period (s)	U*cw	U*wm	U*c
7/17/03	3:59	1.57	7.14	10.2	8.0	6.2
7/17/03	4:59	1.57	6.67	10.0	7.9	6.2
7/17/03	5:59	1.58	6.67	10.0	7.9	6.2
7/17/03	6:59	1.52	6.67	9.9	7.7	6.2
7/17/03	7:59	1.55	6.25	9.7	7.6	6.1
7/17/03	8:59	1.34	6.67	9.4	7.2	6.1
7/17/03	9:59	1.39	6.67	9.5	7.3	6.1
7/17/03	10:59	1.41	6.67	9.6	7.4	6.1
7/17/03	11:59	1.39	6.67	9.5	7.3	6.1
7/17/03	12:59	1.38	6.67	9.5	7.3	6.1
7/17/03	13:59	1.3	6.67	9.3	7.0	6.1
7/17/03	14:59	1.2	7.14	9.2	6.9	6.1
7/17/03	15:59	1.19	5.88	8.7	6.4	5.9
7/17/03	16:59	1.2	6.67	9.0	6.7	6.0
7/17/03	17:59	1.23	6.67	9.1	6.8	6.0
7/17/03	18:59	1.22	6.67	9.1	6.8	6.0
7/17/03	19:59	1.1	6.67	8.8	6.4	6.0
7/17/03	20:59	1.1	6.67	8.8	6.4	6.0
7/17/03	21:59	0.99	6.25	8.4	5.9	5.9
7/17/03	22:59	0.93	6.25	8.3	5.8	5.9

VITA

Edward James Majzlik was born on 10 October 1979 in Aiken, South Carolina. He attended the University of South Carolina from 1998 to 2002 and earned a Bachelor of Science degree in Marine Science in May 2002. He received a Master of Science degree in Oceanography from Texas A&M University in May 2005. His permanent address is 2131 Dibble Rd, Aiken, South Carolina 29801.